2013

The Effect of Temperature on the Electrical and Optical Properties of p-type GaN

Joy McNamara
Virginia Commonwealth University

The Effect of Temperature on the Electrical and Optical Properties of p-type GaN

A Thesis submitted in partial fulfillment of the requirements for the degree of Master of Science in Physics and Applied Physics at Virginia Commonwealth University.

By:

Joy Dorene McNamara

B.S. Physics, Virginia Commonwealth University, 2011

Directors:

DR. MICHAEL A. RESHCHIKOV

ASSOCIATE PROFESSOR, DEPARTMENT OF PHYSICS

&

DR. ALISON A. BASKI

PROFESSOR, DEPARTMENT OF PHYSICS

Virginia Commonwealth University

Richmond, Virginia

May, 2013

Acknowledgments:

Significant accomplishments in life are indubitably the result of many individuals who collectively contribute to the overall success of any achievement. I am compelled to say that earning my Master's degree in Physics is by no means the exception! Thus, I am thrilled to extend my heartfelt gratitude to those responsible in part - great or small – to the completion of this work.

Dr. Michael Reshchikov (a.k.a. "boss-man", "the Machine"), I truly cannot express how blessed I am to be your student. For the countless hours you have spent training me and explaining difficult concepts to me, you should be paid in gold. For being so incredibly patient with my slow brain, and allowing me to frequently visit you in your office to "bother" you, you deserve a very special prize. For carefully and competently assisting me in my development into a proficient scientist, like you, you have my highest respect! I believe that the most important lesson you have taught me is the value of numbers: plugging them in, analyzing them, plotting them, and understanding orders of magnitude. I think this is one of the keys to your genius, and I am so grateful that you have shared it with me. I am so excited that I have the privilege of being able to spend three more years researching with you and learning from your brilliance. Someday, you will be famous, and I'll get to say, "Yes, that's my boss!" Thank you for everything!!

Dr. Alison Baski, you truly are my "physics mom"! From the very first day I came to VCU, you have guided me and nurtured my development in academics and research. Without you, I am confident that I would have been lost in the vastness of VCU. However, because of your competent leadership skills, vast knowledge, and very logical, organized brain, I have been able to achieve many things and become a capable physicist. I am so thankful for the numerous office visits (even some late at night), the red "love marks" on all my writings, sponsoring me for Toastmasters, cookies from Panera, and most importantly, the opportunity to expand my horizons at conferences including my very first international conference in Tampa, FL. I greatly respect your many achievements and believe that as a result of your influence, I am learning to be a confident woman in a professional and scientific environment. You are a very special person in my life, and I am overflowing with gratitude for all you've done for me. I am looking forward to learning so much more from you in the coming years. Thank you!!

Dr. Michael Foussekis, I think you know how much you are responsible for all of this! I am so grateful for the two years you spent training me and putting up with me as a constant "sidekick". I learned so much from working with you, and I am grateful for all the opportunities you provided to me. I am trying to take good care of the Kelvin probe for you, and maybe someday, I'll be able to train somebody else with the same level of excellence which you gave to me! I miss you being here at Physics, but I am so happy for all the things you have accomplished in your career. Thanks for everything Mikee!

To all my professors at the Physics department and elsewhere at VCU, you deserve an award for all the things you do for your students! I'm so thankful especially to Dr. Bishop, Dr. McMullen, Dr. Khanna, Dr. Bertino (for all the caffès!), Dr. Morkoç, Dr. Jason Arnold, and Mrs. Faye Prichard for pouring your knowledge into me and for investing so much time into my learning. Without you, I couldn't have made it! I'm so thankful for Mrs. Janice and Mrs. Evelyn for mothering all of us Physics students and especially since you are the reason I got into research in the first place. I love you both so very much!

To all my friends at physics: Lauren, Nahli, Anita, Iwona, Monica, Joe, Louis, Karen, Skrobbs, Kevin L., Vince, Chris A., Anthony, Ibrahima, Rosy, Ebtihaj, Marissa and Crystal Autumn, you make the Physics department an amazing place! Thanks for all the study times together, and study breaks and chats. I love how we can all commiserate together and how we truly do understand each other. Only VCU physics students can truly appreciate the effort behind our Physics degree. You've been there and earned it too! Congratulations!

To my best friends, Olivia and Reena, I can't begin to tell you how important you are to me! You are an incredible blessing and you've kept me sane these many years. I am excited to see where your careers will lead you. I am so thankful for you! I love you most!

Finally, I owe an enormous amount of gratitude to my wonderful and loving family. I have the best four brothers and sister in the world. Dave and Peter taught me to be strong, Ruthie taught me to be a tough but girly girl, Joel is my twin and "partner in crime", and Danny is my protégé and very special baby brother. I love each one of you, and I am so blessed to be in the middle! To my sister-in-law Muy Muy, thanks for keeping me in shape with all that gym time. You're the best running buddy! To my brilliant Mom and Dad, thank you for teaching me all these years, not just in academics but in all the important life decisions. Thank you so much for encouraging me and pushing me to pursue my dreams. Thank you for your loving support and for enabling me to be who I am today! You are my heroes and I thank God daily for you! I love you so very much!

Now to the One who is worthy of all praise and glory and Who is truly the source of all good things, to my Savior and Lord, I humbly present these meager and human efforts for Your glory alone. "I can do all things through Christ who gives me strength." "When I am weak then I am strong, because the power of Christ rests upon me." Thank you for carrying me and empowering me and for bearing me on wings like eagles. Soli Deo Gloria. Glory to God alone!!!

Table of Contents

List of Figures (captions):

Abstract:

The Effect of Temperature on the Electrical and Optical Properties of p-type GaN

By Joy Dorene McNamara

A Thesis submitted in partial fulfillment of the requirements for the degree of Master of Science in Physics and Applied Physics at Virginia Commonwealth University.

Virginia Commonwealth University, 2013

Major Directors:

Dr. Michael A. Reshchikov

Associate Professor, Department of Physics

&

Dr. Alison A. Baski

Professor, Department of Physics

The development of gallium nitride (GaN) light emitting devices has reached extraordinary echelons. As such, the characterization and analysis of the behavior of GaN materials is essential to the advancement of GaN technology. In this thesis, the effect of temperature on the optical and electrical properties of p-type GaN is investigated. The GaN samples used in this work were grown by various methods and studied by Kelvin probe and photoluminescence (PL) techniques. Specifically, the surface photovoltage (SPV) behavior and PL data were analyzed at different temperatures and illumination intensities. Using the SPV results, we show that p-type GaN exhibits n-type conductivity at low temperatures (80 K). If the sample is heated beyond a characteristic temperature, T_C, the conductivity reverts to p-type. This temperature of conversion can be tuned by varying the illumination intensity. We explain this conductivity conversion using a simple, one-acceptor phenomenological model. Temperature-dependent PL measurements taken on Mg-doped p-type GaN layers show abrupt and tunable thermal quenching of the PL intensity. This effect is explained by a more complex model but with the same assertions, that the system must undergo a change in conductivity at low temperatures and under UV illumination. It is necessary to understand the observed behaviors, since the implications of such could have an effect on the performance of devices containing *p*-type GaN materials.

Chapter 1: Introduction to Material System

1.1 Motivation

Energy usage and consumption are vastly important issues that, if left unaddressed, could have devastating effects on society and our world. Perhaps the most luminous manifestation of our energy usage is lighting. In 2012, the U.S. Department of Energy reported that lighting comprised 7% of the total energy and 18% of the total electricity consumed in the U.S in 2010.[1] With pressing energy concerns, it is essential that alternative forms of energy are produced and utilized; by necessity, this includes exploring alternative forms of lighting.

Light emitting diodes (LEDs) have become increasingly popular for lighting displays. In particular, gallium nitride (GaN) LEDs have elicited enormous attention due to their high-brightness and brilliant blue emissions (**Figure 1a**). Nearly twenty years ago, Shuji Nakamura and his team produced the world's first GaN LED with a p-n junction. The external quantum efficiency of the blue LED has grown over the past twenty years from 0.1% to over 55% with revenues peaking above billions of dollars per year. Now, this wide-bandgap, semiconductor-based device has infiltrated a variety of lighting applications, including TVs, cellular devices, car headlights, streetlights, and numerous other lighted objects.

It has been postulated that the use of GaN LEDs could reduce worldwide electricity consumption for lighting by more than 50%. Yet, there are major issues that must be dealt with before this goal can be attained. These include cost reduction of commercial production, determining the cause of the "efficiency droop" in green LEDs, and in some cases resolving the problem of lattice mismatch between GaN epitaxial layers and sapphire substrates which causes inherent stress and dislocations. These factors affect the LED efficiency, lifetime and cost

advantage. Consequently, research on GaN materials and GaN based devices is desperately needed to resolve such issues.

a.  b. 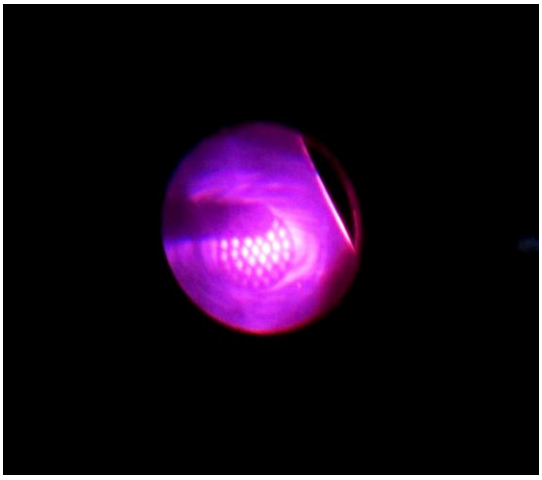

Figure 1: (**a**) A GaN light emitting diode. (**b**) The photoluminescence of a GaN thin film at low temperature as a laser passes through a perforated metal probe before shining on the sample in our Kelvin probe setup.

1.2 Gallium nitride

Gallium nitride is a binary compound consisting of Ga and N atoms. The combination of these two elements produces a wide-bandgap semiconductor with a wurtzite crystal structure (**Figure 2**) and a high melting point. It is most commonly deposited in the form of thin layers on sapphire or silicon carbide substrates. Because of its optical properties and wide bandgap, GaN is ideal for lighting and sensing applications, as well as high speed, field-effect transistors. GaN is typically grown by molecular beam epitaxy (MBE), metal organic chemical vapor deposition (MOCVD) or halide vapor phase epitaxy (HVPE). To grow *n*- or *p*-type GaN, a variety of dopants may be used: silicon (Si) or oxygen (O) for n-type, and magnesium (Mg) for p-type. GaN-based compounds usually have a high density of extended defects.

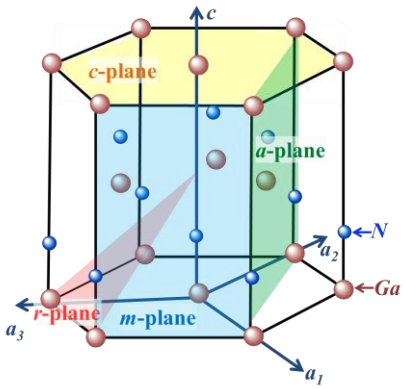

Figure 2: GaN crystal diagram showing the various crystallographic planes.

1.3 Band bending in GaN

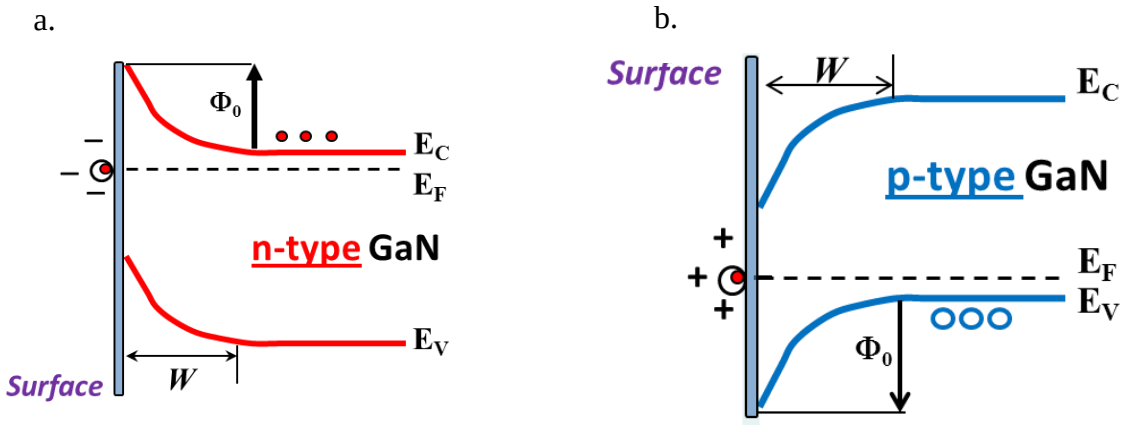

Figure 3: Energy band diagrams for (**a**) *n*-type and (**b**) *p*-type GaN. The band bending in dark is indicated by Φ_0, the depletion region by *W*, and the energy levels of the conduction band, electron Fermi level and valence band by E_C, E_F and E_V, respectively. The band bending is caused by negative and positive charge at the surface, respectively.

Electronic band bending exists at the surface of GaN where all the potentials are bent upwards for n-type GaN and downwards for p-type GaN (**Figure 3**). [2,3,4] The magnitude of the band bending in dark conditions, Φ_0, for *n*-type GaN has been calculated to be about 1.0 eV (Ref. 4) and for *p*-type GaN to be about 2 eV (Ref. 5). The negative (positive) surface charge

responsible for the upward (downward) band bending may originate from defects at the surface such as dangling bonds, lattice mismatch, impurities, or adsorbed species.[6]

1.4 Surface photovoltage

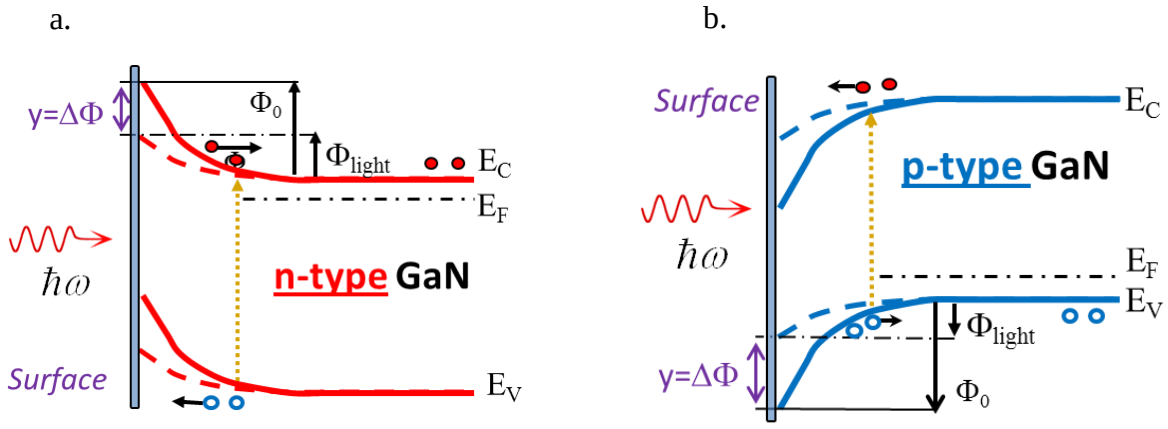

Figure 4: Surface photovoltage, *y*, caused by UV light absorbed in the depletion region. (**a**) For *n*-type, holes swept to the surface decrease the net negaitve charge, thereby decreasing the magnitude of the band bending. (**b**) For *p*-type, electrons swept to the surface decrease the net positive charge, thereby decreasing the magnitude of the band bending. Change in band bending under illumination is defined as the surface photovoltage; *i.e.*, $\Delta\Phi = \Phi_0 - \Phi_{light} = y$.

The surface photovoltage (SPV) technique is an effective characterization tool often used to study and calculate the magnitude of the band bending.[6] Generating an SPV commonly involves illuminating the sample with above-bandgap light to generate electron-hole pairs in the depletion region (**Figure 4**). Due to the strong electric field, electron-hole pairs are very quickly separated, while the electrons are swept to the surface for p-type materials and to the bulk for *n*-type materials (the movement of positively charged holes is always opposite to the movement of electrons in the electric field.) For typical illumination intensities, the overall surface charge is changed almost instantly due to reduction of the excess negative or positive charge at the surface which reduces the magnitude of the band bending.

1.5 Kelvin probe

The Kelvin probe method was first invented in 1861 by the renowned Scottish scientist Lord Kelvin. It is a system in which an oscillating metallic probe is brought near to a conducting surface, and the contact potential difference (CPD) between the two surfaces is measured.[7] By using a Kelvin probe, it is possible to directly measure the change in surface potential as a GaN sample in dark conditions is illuminated with ultraviolet (UV) light. A change in the CPD signal under illumination typically signifies that an SPV has been generated, since SPV is defined as a change in the surface potential (band bending). In dark conditions, the CPD signal is close to zero for GaN when a steel probe is used. Under illumination, the CPD signal almost instantly increases in the positive direction for *n*-type GaN and in the negative direction for *p*-type GaN. In this way, the type of sample conductivity can easily be determined. Additionally, the Kelvin probe uses the position of the Fermi-level in bulk as a reference point, so the position of the Fermi level may also be studied.

1.6 Temperature-dependent surface photovoltage

Temperature-dependent investigations of the SPV behavior have rarely been reported for electronic materials such as GaN. Since temperature greatly affects the transition rates of charge carriers between the surface and the bulk, performing temperature-dependent measurements can clarify the effect of adsorbed species and defects on electrical properties and in particular, the surface band bending. In a few cases, high-temperature studies on *n*- and *p*-type GaN have been conducted; [2, 8] however, to the best of our knowledge, low-temperature SPV studies of GaN have not been reported.

In previous works,[5,8] we measured the temperature-dependent behavior of the SPV for *n*- and *p*-type GaN, at temperatures from 300 to 600 K, and showed that surface band bending is

independent of temperature. In this thesis, we report the results of measurements taken under low temperature conditions for *p*-type GaN grown by various methods. Here, the term "SPV" will be used in a broader sense to describe the "change in CPD" under illumination, although technically, it is defined as a change in band bending under illumination. Later, we will show that a change in the CPD under illumination is not always the result of a change in the surface potential.

1.7 Photoluminescence from defects in GaN

Photoluminescence (PL) is caused by illuminating the sample with above-bandgap light (usually UV for GaN), and is simply the spontaneous emission of light from electronic transitions between defects in the band gap and the conduction band within a semiconductor. The PL may be dispersed with a monochromator, collected by a photomultiplier tube and plotted as the intensity of the emitted light versus energy or wavelength. Measuring and analyzing the PL spectrum from GaN thin films has provided much useful information regarding the properties of defects in GaN.[9] However, the identification of defects and the determination of their exact electronic and spatial structure is still a challenge for experimentalists and theorists. By varying the temperature and the excitation intensity, it is possible to model the behavior of PL from these defects and thereby acquire valuable information regarding the location of defect energy levels, the activation energy, the concentration of defects, the capture coefficients and the characteristic lifetimes of PL through the defects, just to name a few. In this thesis, we report the effect of temperature on the PL from Mg-doped *p*-type GaN.

Chapter 2: Literature Review

Kelvin probe studies are most commonly performed at room temperature, so temperature dependent studies have rarely been reported. In the few cases where measurements are taken at various temperatures, the reported band bending values for *p*-type GaN vary widely.

2.1 High temperature studies of band bending using X-ray photoemission spectroscopy

Bermudez and Long performed photoelectron spectroscopy (PES) to calculate the binding energies of electronic states at the surfaces of *n*- and *p*-type GaN samples.[10] In particular, they examined the effect on SPV of source intensity, sample temperature and chemisorption for both sample types.

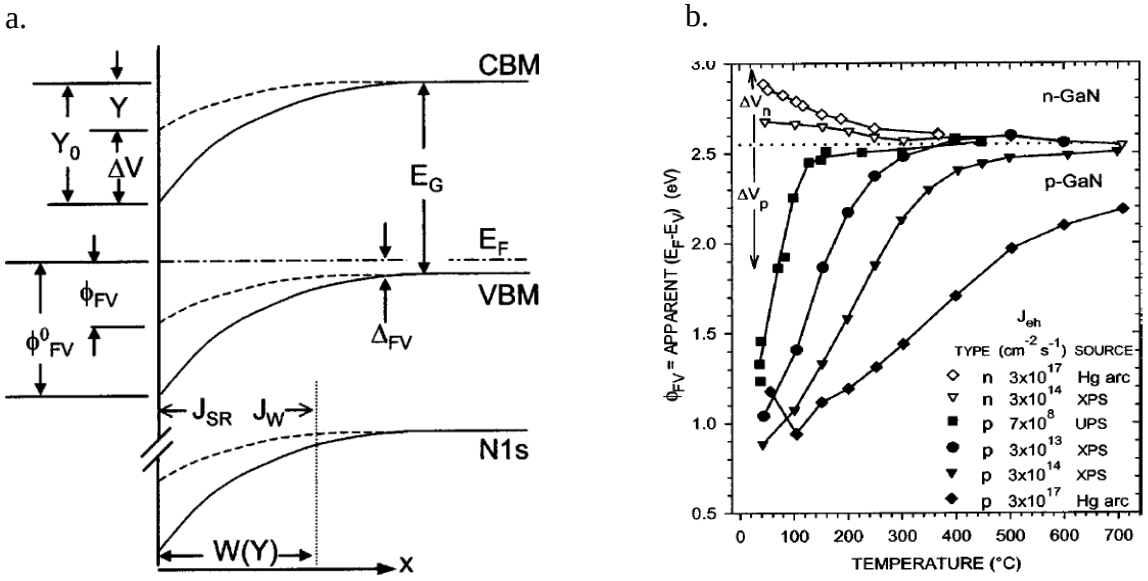

Figure 5: (**a**) Schematic diagram showing the band bending in the dark (solid lines) and under illumination (dashed lines) for *p*-GaN. The band bending *Y*, and shifts in *Y*, i.e., the SPV Δ*V*, are the same for the valence-band maximum (VBM) and conduction-band minimum (CBM) and for all core levels. The J's are electron-hole current densities. (**b**) ϕ_{FV} (defined in **a**) vs increasing *T*, for *n*-(open symbols) and *p*-GaN (solid symbols). The legend gives J_{eh}, the generation rate for *e*-*h* pairs, and the PES source appropriate to each curve. ''XPS'' curves were obtained with different Mg-anode power levels, and ''Hg arc'' refers to XPS data recorded with simultaneous Hg-arc illumination. Smooth curves serve as visual aids. The dotted line at 2.55 eV gives the pinning position common to both types, and $\Delta V_{n,p}$ indicates the respective directions for increased SPV.[10]

The samples studied in this work were grown by MOCVD, cleaned by nitrogen ion bombardment and annealed at ~800 °C, before conducting ultraviolet photoemission spectroscopy (UPS) and X-ray photoemission spectroscopy (XPS) in ultra-high vacuum conditions. To further investigate the SPV, the near-UV flux from a 200 W high pressure Hg-arc lamp was focused on the sample during select PES measurements. Data obtained from the XPS and UPS measurements were fit to estimate the kinetic energies at each temperature of the N 1s, the Ga 3d levels and a grounded Au reference. From these data, the values of the band bending in respect to the Fermi level at the surface were calculated and plotted as a function of temperature and source excitation intensity (**Figure 5**). Their notation differs from ours in that their Y_0, Y and ΔV are equivalent to our Φ_0, Φ and y, respectively.

For *n*-type GaN, we can calculate the band bending from their data, and we find that the value of band bending is nearly independent of temperature but decreases with excitation intensity (0.6 to 0.4 eV, at 40°C). Conversely, the value of band bending for *p*-type GaN increases dramatically for the temperature range, 40 – 700°C, and within the same range, decreases with increasing excitation intensity. For the highest intensity, the band bending increases from -0.7 to -2.0 eV, and for low intensity, it increases from -1.0 to -2.3 eV. Therefore, they report a strong temperature dependence of the band bending in *p*-type GaN. It is of interest, however, that they do not report data taken below 40°C.

2.2 Measuring the work function of *p*-type GaN at low temperature

In a work performed by Eyckeler et al.,[3] the electrical properties at the surface of several *n*- and *p*-type GaN samples were studied as a function of cesium (Cs) coverage, and were investigated at 150 K. From their experimental results, they conclude that on cesiated p-type GaN, a negative electron affinity (NEA) can be achieved. A NEA is a condition where the

vacuum level at the surface drops below the minimum of the conduction band in the bulk. Surface band bending affects the position of the vacuum level at the surface. By manipulating the band bending, they assert that they have indeed achieved NEA conditions.

The details of the experiment are as follows: layers of *p*-type GaN (0001) grown on c-plane sapphire by plasma induced MBE were prepared for this study by standard procedures (dipped in hydrofluoric acid, rinsed with de-ionized water, and annealed at 800 °C). For the deposition of Cs and for all subsequent measurements, the samples were cooled to 150 K. Cs was evaporated onto the surfaces for specific amounts of time, and the coverage as a function of Cs exposure was monitored by XPS. After each period of Cs exposure, a Kelvin probe, operated in dark, was used to monitor the CPD from which the work functions of the samples were calculated. Additionally, the ionization energy of the samples was calculated from the width of the energy distribution curves (EDCs) of the photo-emitted electrons.

In the results, the formation of a Cs layer on the surfaces played an important role in how they interpreted the data. They assert that after a single layer of Cs deposition, core-level shifts must be caused by surface band bending or chemical bonding. Using a Kelvin probe, they first measured the work function for clean *n* and *p*-type surfaces and obtained the values of 3.88 ± 0.15 eV and 3.6 ± 0.15 eV, respectively. As a function of Cs coverage, the work function for both types first decreases then increases to a saturation point (2.1 ± 0.15 eV). They also estimate the ionization energy from the photoemission spectra. For both clean sample types, they calculate a value of 6.8 ± 0.1 eV for the ionization energy. With increasing Cs coverage, however, the ionization energy and correspondingly, the electron affinity decrease to 4.5 ± 0.15 eV and 1.05 ± 0.15 eV, respectively.

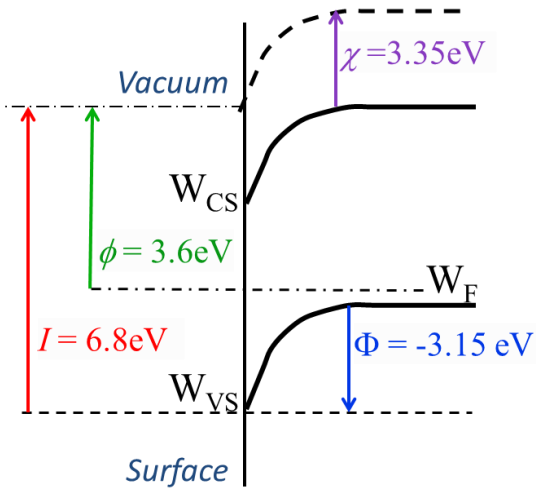

Figure 6: Schematic of energy levels for clean *p*-type GaN as described by Eyckler et al. Values are mostly quoted in the text with the exception of Φ = -3.15 eV being calculated from their values and from reasonable assumptions.

From these results, we may make some calculations concerning the band bending for clean *p*-type GaN. In **Figure 6**, we have drawn the energy levels as per their definitions. Included on the diagram is our calculation of the band bending and various values which they quote in the text based on their EDC's and Kelvin probe measurements. By their definition, the electron affinity, χ, is the energy difference in the ionization energy, I, and the band gap, E_g; *i.e.*, $\chi = I - E_g$. Using E_g = 3.45 eV for GaN, they conclude that χ = 3.35 ± 0.1 eV. As was mentioned previously, they measured the work function, ϕ, to be 3.6 ± 0.15 eV. From the values of the work function and the ionization energy, they calculate that the position of the Fermi level above the valence band is 3.22 eV for *p*-type GaN. From their assumptions that the energy difference between the Fermi level and the valence band in the bulk is 0.05 eV, we calculate a band bending value, Φ, of -3.15 eV. This is the calculated value of band bending at 150 K.

In chapter 6, we will investigate the effect of UV illumination at low temperatures and how this could affect their measured values of the band bending, to show if such large values of band bending are reasonable at 150 K and after UV illumination.

2.3 Low-temperature photoluminescence studies of *p*-type GaN

Although not directly related to the SPV behavior and band bending in *p*-type GaN, temperature dependent PL studies can provide useful insight into the electrical and optical properties of the bulk in high resistivity or Mg-doped *p*-type GaN.

PL studies of high-resistivity Zn-doped GaN layers report for the first time an abrupt and tunable thermal quenching of the PL intensity.[11] For the high-resistivity Zn-doped GaN layers, the PL intensity of the blue luminescence band decreases by two orders of magnitude within a very small temperature range (~10 K) at a characteristic temperature, T^*. By varying the excitation intensity, T^* is tunable. This abrupt quenching was preliminarily attributed to the presence of a certain type of nonradiative defects. Using a phenomenological model, the tunable and abrupt quenching of PL is explained by the temperature-dependent efficiency of capture for free carriers by various radiative and non-radiative defect sites. For temperatures below T^*, the sample is predicted to undergo a conductivity conversion due to the very efficient recombination of free carriers via a non-radiative defect. If a conversion of the conductivity does indeed occur for some *p*-type GaN samples, it may have interesting effects on the SPV behavior at low temperature.

2.4 Main results from the literature and unsolved problems

A few works have studied the effect of high temperature on the SPV behavior in *p*-type GaN, while none have studied the effect of low temperature on the SPV behavior. The most important of these reviewed works appears to be the low temperature PL studies which predict very interesting behavior at low temperatures. In this thesis, we will present both published and unpublished data from our studies of the SPV behavior for *n*- and *p*-type GaN in a wide range of

temperatures. While explaining the results of our data, we may be able to solve some of the existing problems and discrepancies in the literature regarding low temperature studies of *p*-type GaN.

Chapter 3: Experimental Details

The primary instruments used in this work were a Kelvin probe system (McCallister Technical Services, KP6500) and a custom-built photoluminescence setup.

3.1 Kelvin probe setup

The Kelvin probe method is a very sensitive technique used to detect small changes in the surface potential of materials. Specifically, it measures the CPD between a probe and a sample, which are electrically connected, by monitoring the difference in the work functions of the sample and the probe, while a backing voltage is applied to the probe. Since the surfaces of the probe and sample are parallel to each other, a capacitance is established between the two materials as in a parallel plate configuration. The probe oscillates in reference to the stationary sample to vary the capacitance, and the change of the potential difference in time across the sample and the probe is monitored as a function of the backing potential. When no external backing potential is applied, the CPD is simply the difference of the work functions of the metal probe, ϕ_m, and sample, ϕ_S:[12]

$$qV_{CPD} = \Delta\phi = \phi_m - \phi_S \tag{3.1}$$

Since the probe is oscillating, the capacitance between the two plates will be varying as a function of time, in a sinusoidal manner. The charges on the plates are kept in equilibrium, since they are connected in circuit and the current is free to flow between the plates. When the backing potential applied to the probe is equal to the negative CPD on the surface of the sample (*i.e.*, $V_{Backing} = -V_{CPD}$), then the field between the two plates will be equal to zero. Thus the induced charge is also zero, requiring that the current also vanish. This balance point is called the "null point", and is precisely how the CPD is determined. [12]

The measured signal of the Kelvin probe is the current flowing between the probe and the sample, and is dependent on the distance of separation between the two plates, d_0, the oscillation amplitude of the probe, d_1, and the frequency of oscillation of the probe, ω.[12] The capacitance for a parallel plate capacitor is known to be,

$$C = \frac{\varepsilon\varepsilon_0 A}{d} \tag{3.2}$$

Here, A is the area of the parallel plate, and d is the separation distance between the plates. If we assume a sinusoidally varying separation, and an arbitrary phase ϕ, [12]

$$d = d_0 + d_1 \sin(\omega t + \phi)\,, \tag{3.3}$$

and by using the relationship,

$$i = \frac{dQ}{dt} = \Delta V \frac{dC}{dt}\,, \tag{3.4}$$

where ΔV is the difference in potential between the probe and the sample, then the current is given as,[12]

$$i = -\varepsilon\varepsilon_0 A \Delta V \frac{d_1 \omega \cos(\omega t + \phi)}{[d_0 + d_1 \sin(\omega t + \phi)]^2}\,. \tag{3.5}$$

It is interesting to note that in Eq. (3.5), the current is zero when the difference in potential, ΔV, goes to zero which we have defined as the "null point". The Kelvin probe software scans through a positive and negative backing potential value (e.g., +2 V and -2 V) and measures the resulting current amplitude at these points. Plotting the current amplitudes (also known as the peak-to-peak values) versus the backing potential yields a linear relationship. The x-intercept of this line is where the current is zero, the difference in potential of the probe and sample is also

zero, and thus the point at which the backing potential exactly cancels the value of the CPD (the "null point"). Thus, the CPD can be interpolated from the linear relationship of the current amplitude versus backing potential.[12]

a.

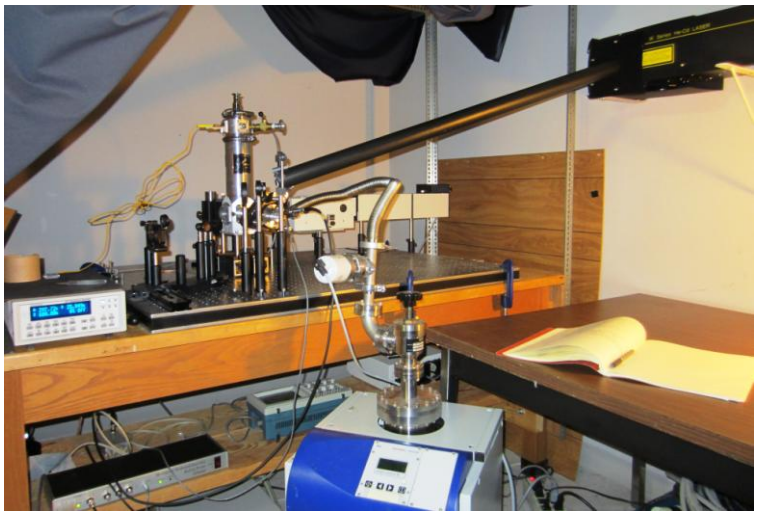

b.

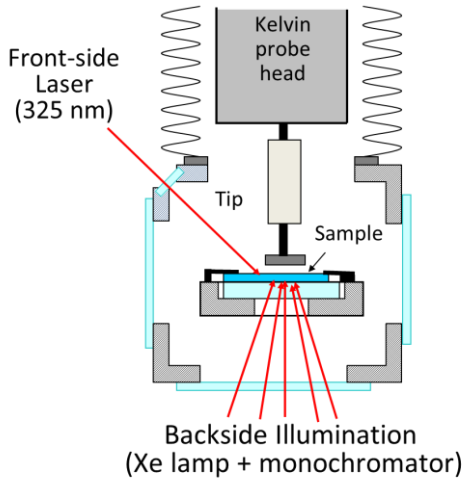

Figure 7: (**a**) A picture of the setup of the Kelvin probe system, and (**b**) schematics of the probe and sample configuration. Both excitation sources have a maximum intensity of P_{exc} = 30 mW/cm^2.

The experimental setup (**Figure 7**) used to perform SPV measurements consists of a Kelvin probe (KP-5600 from McAllister Technical Services) attached to an optical cryostat (VPF-700 from Janis Research Co., Inc.). The cryostat is multifunctional with the ability to

operate at low and high temperatures ($T \approx 80 - 600$ K), in high vacuum (base pressure ~ 10^{-6} mbar) or in a gas/air ambient, and allows for illumination from either the back (Xe lamp and monochromator) or the front side (HeCd laser) of the sample. The samples in this work were illuminated with the front-side geometry by a laser beam (HeCd, 325 nm) with a maximum power density $P_0 \approx 30$ mW·cm^{-2}. The laser beam passed through a window in the cryostat and a perforated metal probe (4 mm dia.) before shining on the sample.

3.2 Photoluminescence setup

The setup used to collect PL data was custom built and is shown in **Figure 8**. For our excitation source, we use a UV (325 nm) HeCd laser with a total power of 50 mW. The laser beam is directed through a set of filters to the sample which is mounted on a holder within a cryostat. The filters enable us to attenuate the power density that is incident on the sample and to filter out any parasitic lines. In this way, we are able to study the intensity dependence of the PL. When the UV light hits the sample, PL is spontaneously emitted in all directions, and a small portion of the emitted PL is collected by a series of lenses called the condenser. The captured light is directed by the condenser towards a monochromator. The light entering the monochromator is sorted into the various wavelengths using a grating inside the monochromator. The grating can be rotated, so that different wavelengths can be chosen to exit the monochromator. In this way, we can measure the PL intensity as a function of the photon energy or the wavelength. Outside of the monochromator, the light is detected by an attached photomultiplier tube (PMT), and the electronic signal is then discriminated by the photon counting system. Finally, the data is output to the computer system.

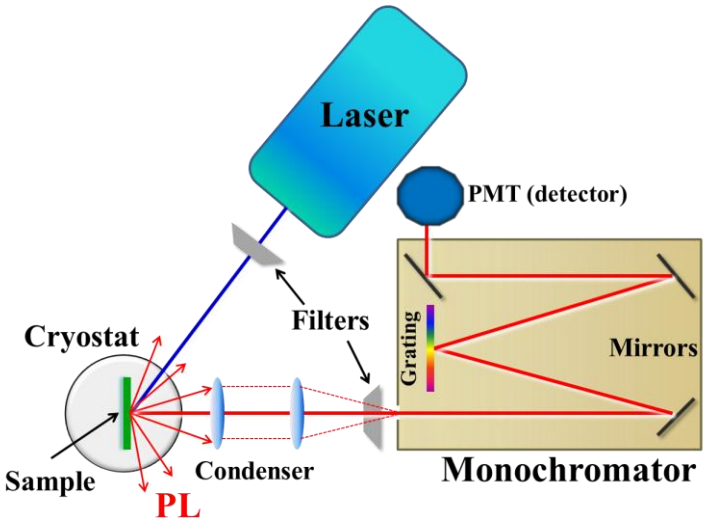

Figure 8: Schematics of the PL setup, including excitation source (HeCd laser, sample and cryostat, condenser, monochromator and PMT detector.

3.3 Gallium nitride samples

Three *p*-type GaN samples were studied for the majority of this work. The samples were grown by various techniques: metalorganic chemical vapor deposition (MOCVD, sample 983), halide vapor phase epitaxy (HVPE, sample 863) and molecular beam epitaxy (MBE, sample 9591). Hall effect measurements were used to determine carrier type and concentration; however, the results were mostly ambiguous, apparently due to a degenerate *n*-type layer close to the GaN sapphire interface.[13] As was mentioned previously, SPV measurements are able to determine the type of conductivity, and they do confirm the *p*-type nature of these samples, at room temperature. Hot probe measurements also indicate that the samples have *p*-type conductivity. Additionally, the SPV data collected from an undoped *n*-type GaN sample, grown by HVPE (by Ostendo Instruments – TDI) will be analyzed for comparison. For all the samples

studied in this work, Ohmic contacts were formed by depositing Ni/Au layers around the sample periphery.

3.4 Surface photovoltage measurement procedures

Prior to any SPV measurement, the samples were kept in dark and heated to 600 K for one hour, then subsequently cooled to the desired temperature in dark to allow for complete restoration of the band bending. A secondary method of sample preparation, not frequently used in this study, is to allow the sample to restore in dark for about 1 day at 295 K. For low-temperature measurements, the sample holder was cooled with liquid nitrogen to $T \approx 80$ K, and the temperature of the sample was allowed to stabilize before taking data. SPV measurements were performed for the temperature range 80 – 300 K (intervals of 10 K) with 5 min of UV illumination at each temperature. Additionally, 5 – 7 min were allowed at each temperature interval for a brief restoration and for heating to the next desired temperature.

Chapter 4: Surface Photovoltage in *n*-type GaN

The investigation into the temperature-dependent behavior of the SPV began on *n*-type GaN samples. The initial studies entailed mostly high temperature experiments where the transient SPV behavior, the intensity dependent SPV behavior, the restoration of the SPV signal after UV illumination and the true value of surface band bending for various temperatures were all examined. To interpret the SPV behavior at low temperatures and for *p*-type GaN, it is necessary to first understand the SPV behavior of *n*-type GaN and as a function of temperature.

4.1 Modeling the surface photovoltage

N-type GaN exhibits upward band bending at the surface by approximately 1 eV due to negative surface charge (**Figure 3a**).[2,4,8] Illuminating a sample with UV light reduces the band bending in dark, Φ_0, to some value Φ, which results in a surface photovoltage, $y = \Delta\Phi = \Phi_0 - \Phi$ (**Figure 4a**) Under UV illumination, electron-hole pairs are created in the depletion region near the surface and are quickly separated due to a very strong electric field. For *n*-type, electrons are swept to the bulk while holes are swept to the surface, which add positive charge to the surface and reduce the band bending. The initial negative charge at the surface may be the result of adsorbed species or semiconductor and interface states which arise from disorder, dangling bonds, point defects, etc.[4] In this case, photo-generated holes can very quickly change the density of charge at the surface, which results in the reduction of band bending. Over time, photo-induced absorption or desorption of charged species may enhance this process, but for this particular discussion, we defer this to another work.[4] For simplicity, all of the holes generated by the UV light in the depletion region reach the surface and recombine with surface electrons to reduce the band bending.[4]

Apart from the photo-induced transitions, thermionic transitions between the surface and the bulk are also present and may be described in terms of Boltzmann statistics. Surface states may trap free electrons from the bulk which have overcome the near-surface barrier, and conversely, electrons trapped at the surface may escape over the barrier to the bulk region. The flow of electrons from the bulk to the surface is defined as,[4]

$$R_{BS} = s_n N_C \exp\left(-\frac{\Phi_0 + (E_C - F) - y}{kT}\right). \tag{4.1}$$

Here s_n is the surface electron recombination velocity, N_C is the effective density of states in the conduction band, Φ_0 is the dark value of band bending, $(E_C - F)$ is the position of the bulk Fermi level in respect to the conduction band minimum, y is the surface photovoltage, k is Boltzmann's constant and T is the temperature.

The rate of electrons flowing from the surface to the bulk is similarly described as,[4]

$$R_{SB} = s_n N_C \exp\left(-\frac{E_C - E_S}{kT}\right), \tag{4.2}$$

The energy state from which the electrons are emitted is defined as E_S and may be considered as discrete or continuous. If the Fermi level in the bulk is pinned by this surface state, then the value of band bending in dark is dictated by the relationship, $E_C - E_S = \Phi_0 + (E_C - F)$.[4]

Once the illumination has ceased, the band bending begins to restore as the SPV, y, decays to zero, from the time $t = 0$ to $t \to \infty$. A simple analytical expression for the decay of the SPV as a function of time has been derived from a thermionic model to be,[4]

$$y(t) \approx y_0 - \eta kT \ln\left(1 + \frac{t}{\tau}\right). \tag{4.3}$$

In this expression, η is an ideality factor and is assumed to be equal to 1, t is the time from when the illumination is turned off, and τ (Ref. 4) is a time-delay constant which has an exponential dependence on the value of the band bending immediately after illumination. By inspecting Eq. (4.3), it can be seen that the SPV decays with a logarithmic dependence on time. Also, the rate of the restoration is proportional to temperature.

4.2 Temperature-dependent studies of the surface photovoltage

The SPV as a function of temperature and intensity was investigated for a Si-doped, *n*-type GaN film grown by HVPE on a c-plane sapphire substrate with a thickness of approximately 5 μm. From temperature-dependent Hall effect measurements, the concentration of free electrons, n, was estimated to be 3×10^{17} cm^{-3} at room temperature.[8] Prior to any measurement, the sample was kept in dark for approximately one day for $T < 500$ K, or for 1 hour for $T > 600$ K.

The intensity dependent SPV measurements were performed by varying the light intensity with a series of neutral density filters in the order of low to high intensity. The dependence of the SPV on intensity is modeled by the expression:[4]

$$y_0 = \eta kT \ln\left(1+\frac{cP_0}{R_0}\right) \tag{4.4}$$

where c is a geometrical factor which is a fraction of the photons absorbed in the depletion region, P_0 is the excitation intensity and R_0 is the rate at which charge carriers move from the bulk to the surface over the barrier in dark conditions. From Ref. 4,

$$R_0 = s_n N_C \exp\left(-\frac{\Phi_0 + (E_C - F)}{\eta kT}\right) \tag{4.5}$$

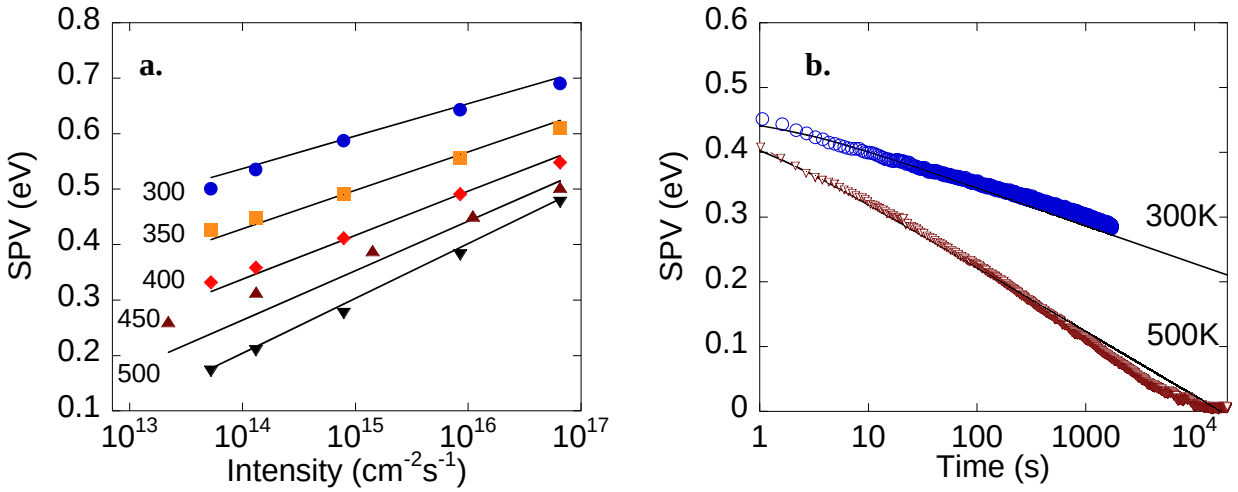

Figure 9: (**a**) Intensity-dependent SPV measurements of *n*-type GaN in vacuum taken at various temperatures using UV illumination (325 nm). Solid lines are calculated using Eq. (4.4) with the parameters: η = 1, c = 0.454 and R_0 = 3×10^4, 3×10^7, 2×10^9, 5×10^{10}, and 4×10^{11} cm^{-2} s^{-1} for T = 295, 350, 400, 450, and 500 K, respectively. (**b**) SPV restorations in vacuum after short (1 s) UV illuminations while at 295 and 500 K at P_0 = 10^{17} cm^{-2}s^{-1}. The fits are calculated using Eq. (4.3) with y_0 = 0.62 and 0.45 eV; Temperature = 300 and 500 K; η = 1; and τ = 0.002 and 0.5 s, respectively.[8]

Here, s_n is the surface electron recombination velocity. By varying the excitation intensity and plotting the dependence of the SPV on intensity, the band bending can be calculated for measurements performed for a range of temperatures. For each measurement, the amount of UV exposure time was limited (~30 and 3 s for low and high intensity, respectively) so as to avoid secondary processes, such as photo-induced desorption or adsorption.

The intensity dependent SPV data for a range of temperatures are shown in **Figure 9a** and are fit using Eq. (4.4). The SPV increases logarithmically with intensity in accordance with the model. For any given intensity, the magnitude of the SPV is higher at lower temperatures, since the rate of R_0 exponentially decreases with decreasing temperature. For select temperatures (300 and 500 K), the restorations of the SPV after illumination has ceased are shown in **Figure**

9b and the data are fit with Eq. (4.3). According to the thermionic model, the SPV restores with a rate that has a logarithmic dependence on time, and increases linearly with temperature. Thus, the restoration of the band bending after illumination has a strong temperature dependence, since at 500 K, the SPV has restored within 3 h, but for 300 K, the SPV may need years to fully restore.

Furthermore, experiments agree with the thermionic model since by preheating the sample to 600 K and allowing the band bending to restore for 1 h at such high temperatures before any measurement yields more accurate baselines for the intensity dependent measurements. From these measurements, consistent values of the band bending can be calculated from the experimentally obtained R_0 values [from Eq. (4.4)] and in conjunction with Eq. (4.5). By using the R_0 values in the caption of **Figure 9**, the band bending is estimated to be 1.05 ± 0.04 eV for the temperature of 295 – 500 K.[8]

By analyzing the behavior of the surface photovoltage in *n*-type GaN, we have determined both theoretically and experimentally that the restoration of the band bending has a strong temperature dependence, such that to obtain accurate and consistent values of band bending, the sample must be allowed to restore in dark at high temperatures if restoration is to be attained in a reasonable amount of time.

Chapter 5: High-Temperature Studies of the Surface Photovoltage in *p*-type GaN

Due to the success of accurately estimating the value of band bending in *n*-type GaN by studying the temperature dependence of the SPV, it was assumed that *p*-type GaN should exhibit similar behavior. However, a quick review of the literature shows a very disparate value of band bending for *p*-type GaN ($0.8 < |\Phi_0| < 3.0$ eV).[2, 3, 14] By investigating the reports, it is apparent that experimental conditions do greatly affect the measured value of the band bending.

5.1 Surface photovoltage in *p*-type GaN at high temperatures

P-type GaN exhibits downward band bending due to excess positive charge at the surface (**Figure 3b**). By illuminating with band-to-band (UV) light, electrons in the depletion region which are excited to the conduction band are very quickly swept to the surface by the strong electric field. The increase in the negative surface charge reduces the magnitude of the downward band bending, and results in a SPV (since $\Delta\Phi$ = SPV) (**Figure 4b**). After illumination, the rate of restoration for the band bending has a logarithmic time dependence and increases with sample temperature. Thus, high temperature surface photovoltage measurements are very instrumental in clarifying the disagreement of the reported band bending values in *p*-type GaN.

The band bending in *p*-type GaN can be calculated by fitting SPV data with a thermionic model in a similar fashion to how it is calculated in *n*-type GaN. The value of the SPV, y_0, for p-type GaN can be expressed as,[5]

$$y_0 = -\eta kT \ln\left(\frac{cP_0}{R_0} + 1\right) \tag{5.1}$$

with

$$R_0 = s_p N_V \exp\left(\frac{\Phi_0 - (F - E_V)}{\eta kT}\right), \tag{5.2}$$

where R_0 is the rate at which holes can overcome the near surface barrier and move from the bulk to the surface, s_p is the surface recombination velocity for holes, N_V is the effective density of states in the valence band, and $F - E_V$ is the position of the Fermi level in respect to the valence band maximum. We can write a simpler equation combining both Eqs. (5.1) and (5.2), since the value of cP_0/R_0 is much greater than 1 for the range of light intensities used in this work. The SPV value can then be written as,[5]

$$y_0 \approx \Phi_0 - (F - E_V) + \eta kT \ln\left(\frac{s_p N_V}{cP_0}\right). \tag{5.3}$$

To use this expression to estimate the value of band bending, we can fit the temperature-dependent SPV data shown in **Figure 10**, and by using the following parameters: c = 0.13 (depletion region width is 12nm), $s_p \approx 10^{5 \pm 2}$ cm/s (Ref. 15), and $(F - E_V)$ and N_V vary from 0.20 to 0.23 eV and from 1.6×10^{19} to 5.3×10^{19} cm^{-3}, respectively, within the temperature range of 295 – 650 K. The error in these parameters resides mostly in s_p which gives an error in band bending of only ± 0.2 eV. Note that the magnitude of the SPV should decrease almost linearly with increasing temperature according to Eq. (5.3).

The dependence of the SPV on temperature for constant illumination intensity is shown in **Figure 10**, where the sample was illuminated for ~1 s with $P_0 = 7 \times 10^{16}$ cm^{-2} s^{-1} for the range of temperatures from 295 to 500 K. The SPV was measured with two different sample

preparation methods: SPV measurements were performed at any temperature either with or without preheating the sample in dark, for 1 h at 600 K, to allow for complete restoration of the band bending. The SPV measurements taken without preheat treatment show the magnitude of the SPV increasing with increasing temperature, contrary to what the thermionic model [Eq. (5.3)] predicts. Conversely, the SPV measurements taken after preheat treatment are in good agreement with the model.

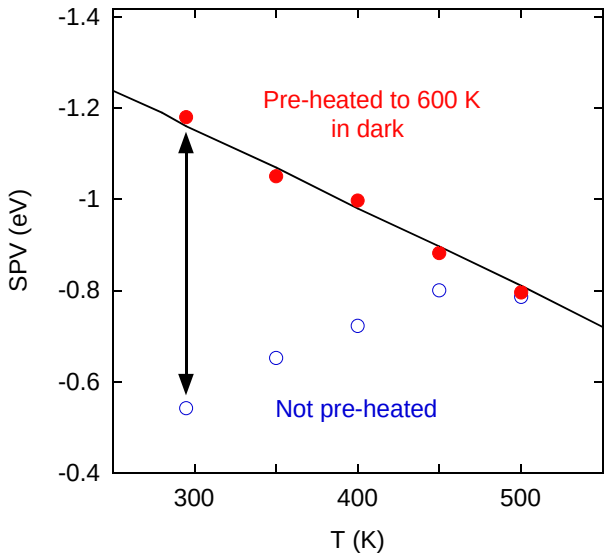

Figure 10: SPV generated with $P_0 = 7\times10^{16}$ cm^{-2}s^{-1} as a function of sample temperature. Sample was pre-heated in dark at 600 K for 1 h (filled circles) or was not pre-heated (empty circles). The solid line is calculated using Eq. (5.3) with the following parameters: $c = 0.13$, $\eta = 1$, $\Phi_0 = -1.45$ eV, and $s_p = 10^5$ cm/s. To find the temperature dependence of F in Eq. (5.3), we used the following parameters: $N_A = 1.3\times10^{19}$ cm^{-3}, $N_D = 6.5\times10^{18}$ cm^{-3}, and $E_A = 0.18$ eV (Ref.5).

At room temperature, there is a very large difference in the magnitude of the SPV between the two methods (indicated by the arrow), even though both measurements were performed at the same temperature and on the same sample. This clearly shows that the band bending was unable to restore within a reasonable amount of time at 295 K, and that preheating the sample is necessary if the true value of band bending is to be measured. Additionally, the very large SPV value of -1.2 eV indicates that the magnitude of the band bending exceeds 1.2 eV at 295 K. From

this data, it is apparent that the restoration of the band bending has a very strong temperature dependence, and that preheating the sample before performing SPV measurements increases the rate of restoration and provides more accurate values of the estimated band bending in dark.

5.2 Calculating the band bending in *p*-type GaN

Now, if we fit the data presented in **Figure 10** by using the parameters given above, with Φ_0 being the only fitting parameter, we find that Φ_0 = -1.45 eV. What is not discussed in great detail in this work is the value of η which is an ideality factor used to fit the experimental data with Eq. (5.3) and whose value should be close to 1. For *n*-type GaN, the value of η is always close to 1, and does not present any error in the calculation of the band bending. However, in *p*-type GaN, the value of η in fitting the intensity dependent SPV data (figure not shown) appears to be temperature dependent. As the temperature increases, the value of η decreases from 3.1 to 1.3. (Ref. 5) The temperature dependence of η may indicate that the high resistivity of the *p*-type samples at low temperatures is causing the Kelvin probe to inaccurately measure the true CPD value. At high temperatures, the conductivity should increase, and simultaneously, so should the ability of the Kelvin probe to accurately measure the CPD. As a result, the band bending values obtained at high temperatures are expected to be more reliable.

An alternative method to calculating the band bending is to use the dark CPD signal of the Kelvin probe. The band bending can be estimated from the following expression:[5]

$$\Phi_0 = \phi_M - \chi - (E_C - F) - qV_{CPD}\,. \tag{5.4}$$

Here, χ is the electron affinity for GaN (3.2 eV from Ref.16), E_g is the bandgap (3.43 eV at 295 K), and qV_{CPD} is the measured CPD signal multiplied by the electron charge. The work function of the stainless steel probe, $\phi_{M,}$ was estimated to be 4.8 eV from the measurement of a

gold foil and 4.45 eV from data for an *n*-type GaN sample with Φ_0 = 1.05 eV.[8] The latter was considered as a more reliable value, because the band bending in this sample was accurately established from SPV measurements by using the thermionic model. In **Figure 11**, the values of the band bending in dark are calculated as a function of temperature (295 – 500 K) for several *p*-type samples (as described in the experimental details section) and for the *n*-type sample discussed in the previous chapter.

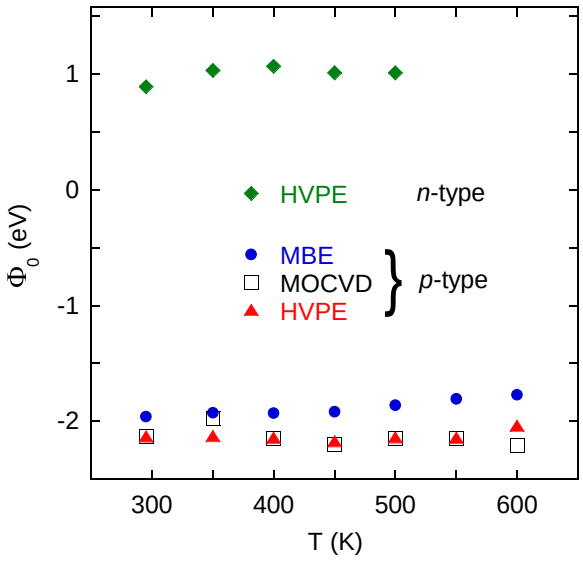

Figure 11: Band bending in dark for both *n*- and *p*-type GaN calculated from CPD measurements in dark using Eq. (5.4) for *p*-type and for *n*-type. The data were obtained after pre-heating the sample for 1 h at 600 K in dark before each measurement.[5]

For all measurements in **Figure 11**, the samples were preheated to 600 K for 1 h to allow for full restoration of the band bending prior to recording the CPD signal in dark. The calculated band bending is obviously independent of temperature and is about -2 eV for all the *p*-type samples studied.

5.3 Modeling the restoration of the surface photovoltage

Furthermore, the restoration of the SPV after illumination at various temperatures shows that the rate of restoration increases with increasing temperature. In **Figure 12**, the restorations of the SPV after short (1 s) illuminations at temperatures 295 K to 500 K are shown. The time required for the band bending to fully restore has a logarithmic dependence and the model is similar to the *n*-type GaN model in the previous chapter. The decay of the SPV can be fit by the thermionic model,[4]

$$y(t) \approx y_0 + \eta kT \ln\left(1 + \frac{t}{\tau}\right), \tag{5.5}$$

with,

$$\tau = \frac{\eta kT}{R_0} \frac{p_s(0)}{2\Phi_0} \exp\left(\frac{y_0}{\eta kT}\right), \tag{5.6}$$

where y_0 is the SPV after illumination has ceased, t is the time elapsed after illumination, τ is a characteristic time delay which exponentially depends on the near-surface barrier, and $p_s(0)$ is the net density of positively charged states at the surface. Equation (5.5) is a simplified version of the restoration equation from a previous work, and it does not account for the complete restoration of band bending.[4] This equation is only meant to predict the behavior at the beginning of restoration and the slope. For this reason, there is no asymptotic behavior in the fits when the SPV data show complete restoration.

As expected, the fits to the SPV data using Eq. (5.5) indicate that the initial slope of the restoration is faster at higher temperatures. By extrapolating the fit for 295 K, the SPV is predicted to fully restore in approximately 10^8 s (a few years). This takes six orders of magnitude more time than the nearly complete restoration of the band bending at 500 K, which should occur

in about 100 s. From these restoration rates, it is clear that heating the sample in darkness allows band bending values larger than 1 eV to fully restore, thereby providing more accurate baselines for SPV and CPD measurements.

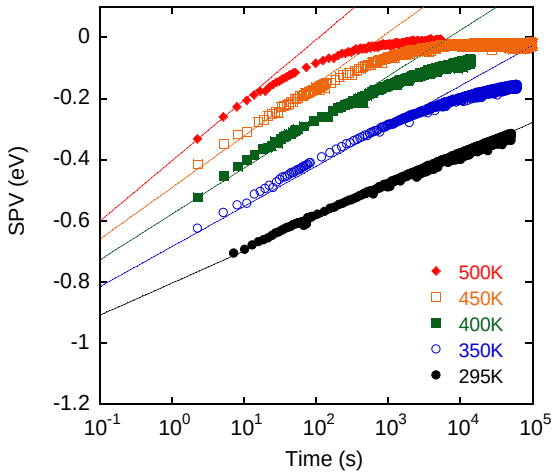

Figure 12: Restorations of SPV after short (1 s) UV illuminations at $P_0 = 7\times10^{16}$ $cm^{-2}s^{-1}$ for temperatures from 295 to 500 K. Each measurement is taken after preheating the sample at 600 K for 1 h. The fits are calculated using Eq. (5.5) with $\tau = 0.001$ s and $y_0 = -1.12$, -1.08, -1.03, -1.0, and -0.9 eV; $\eta = 1.8$, 1.9, 1.9, 1.9, and 2; for $T = 295$, 350, 400, 450, and 500 K, respectively.[5]

From these studies we conclude that the sample temperature greatly dictates the measured value of the band bending, and can explain the wide disagreement in the values of band bending reported for *p*-type GaN in the literature.

Chapter 6: Low Temperature Studies of the Surface Photovoltage

In the previous chapters, we have analyzed the temperature-dependent behavior of the SPV for both *n*- and *p*-type GaN, for the temperature range from 300 to 600 K, and have shown that surface band bending is independent of temperature. Furthermore, it is more accurately estimated when the band bending is allowed to fully restore at high temperatures. In this chapter, we now report the results of measurements taken under low temperature conditions for *p*-type GaN samples grown by various methods.

6.1 Low-temperature surface photovoltage for *p*-type GaN

The *p*-type GaN samples used for these studies were grown by various techniques: MOCVD (sample 983), HVPE (sample 863), and MBE (sample 9591). The experimental setup and procedures are outlined in Chapter 3.

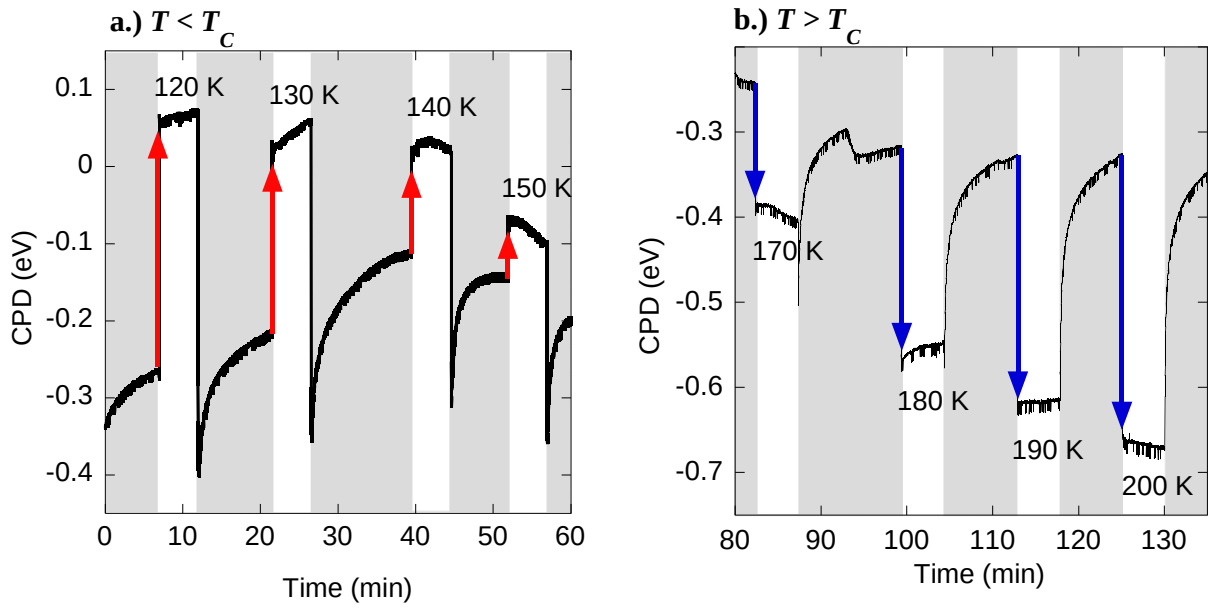

Figure 13: CPD of p-type GaN, HVPE sample 863, at various temperatures, with P_{exc} = 30 mW/cm^2. (**a**) For $T < T_C$, where T_C is the temperature of the conductivity conversion, the SPV exhibits n-type behavior. (**b**) For $T > T_C$, the SPV exhibits p-type behavior. White and shadowed regions represent light and dark conditions respectively. Arrows show the direction of the change in CPD upon illumination.

The real-time CPD at selected temperatures for a representative sample (HVPE) is presented in **Figure 13**. Shadowed and white stripes correspond to dark and illumination conditions, respectively. Arrows indicate the direction of the change in the CPD signal as the sample is illuminated. We can see that at temperatures below 160 K (**Figure 13a**) the CPD increases in the positive direction under illumination, which corresponds to *n*-type SPV behavior. At $T > 160$ K (**Figure 13b**), the CPD increases in the negative direction, which is the expected SPV behavior for *p*-type samples. The temperature at which the direction of the change in CPD switches from positive to negative will hereafter be called the temperature of conductivity conversion, T_C. As the sample is heated to 600 K, the *p*-type behavior remains consistent.

For all three growth types, the change in CPD at 80 K corresponded to *n*-type behavior, while for $T > T_C$ the change in CPD corresponded to normal *p*-type behavior. The measurements were repeated several times and the results were reproducible. The value of T_C varied between 100 and 160 K for different *p*-type GaN samples. Note that in Si-doped *n*-type GaN, the change in CPD corresponded to *n*-type behavior for all temperatures (see **Figure 18**).

The initial value of the SPV (the fast change of the CPD under illumination) for each growth type is plotted in **Figure 14a**. Indicated on the graph is the temperature range in which the MOCVD and HVPE GaN samples demonstrate *n*-type behavior, the characteristic temperature, T_C, at which a conversion to *p*-type behavior occurs and finally, the temperature range in which the samples again exhibit normal *p*-type behavior. For MBE-grown samples, T_C was typically lower – about 100 K.

Furthermore, the effect of excitation intensity on the SPV signal for each sample was investigated. In **Figure 14b**, temperature dependencies of the initial SPV for two different intensities (4 and 30 mW·cm^{-2}) are plotted for the representative MOCVD sample. It is important

to note that T_C (indicated by the temperature at which the data points cross from positive to negative values) shifts to a lower temperature with decreasing excitation intensity. Thus, the temperature of conversion can be tuned by varying the excitation intensity. The shift of T_C to lower temperatures with decreasing illumination intensity was observed for all studied *p*-type GaN samples. Below, it will be shown theoretically that the conductivity type switches from *p*-type to *n*-type under illumination for $T < T_C$, and the temperature of the conductivity type conversion can be tuned by the illumination intensity.

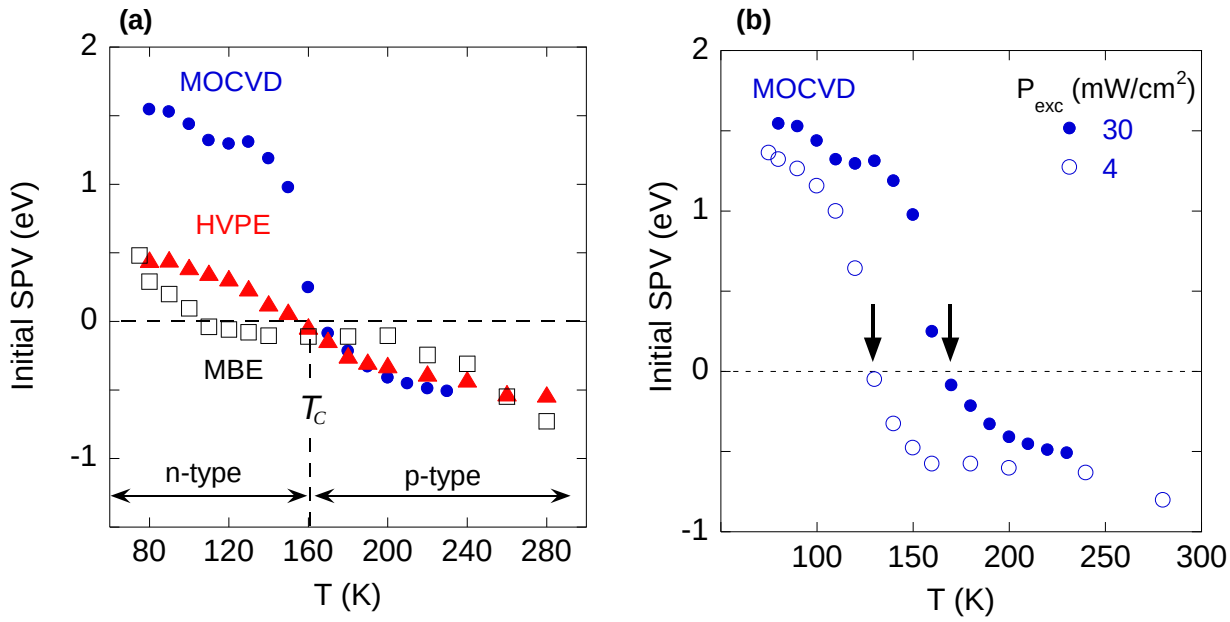

Figure 14: (**a**) Temperature dependence of the initial SPV signal for various *p*-type GaN samples, with $P_{exc} = 30$ mW/cm^2. Temperature T_C, shown for the MOCVD and HVPE-grown samples, indicates the temperature of the conductivity type conversion. (**b**) Temperature dependence of the initial SPV for the *p*-type GaN sample grown by MOCVD for two excitation power densities. Arrows indicate temperatures at which *n*-type conductivity converts to *p*-type conductivity.

6.2 Conversion of conductivity and carrier concentration at low temperature

By studying the low-temperature SPV behavior of *p*-type GaN, we have observed a conversion of the SPV signal from negative to positive with decreasing temperature. This can be

explained by *a conversion of conductivity* from *p*-type to *n*-type. Interestingly, this behavior is observed in three, differently grown, *p*-type samples which all exhibit *n*-type conductivity at 80 K and under UV illumination. From theory, a negative SPV signal is expected for *p*-type samples under UV illumination, since electron-hole pairs created in the depletion region will cause the surface to be flooded with electrons, and the magnitude of the band bending will decrease. At first glance, a positive increase in the CPD signal under illumination (equivalent to a positive SPV signal) observed in *p*-type samples at low temperatures might indicate that the band bending switched from downward to upward as in the case of *n*-type samples. However, it is not reasonable to expect such a flip in the band bending, and it will be shown below that the practical band bending in *p*-type samples at low temperatures is actually very close to zero (less than 0.1 eV downwards), both in dark and under illumination. The unusual effect of the positive increase in the CPD signal at low temperatures can be explained instead by a conversion of the conductivity from *p*-type to *n*-type under illumination, which shifts the electron quasi-Fermi level in bulk towards the conduction band.

To explain the conversion of conductivity, we will use a phenomenological model based on rate equations.[11] In the simplest approximation, let us consider one type of shallow, Mg-related acceptors with concentration N_A and ionization energy E_A that are partially compensated by shallow donors with concentration N_D. The concentrations of the defects in their variously charged states are N_A^-, N_A^0, N_D^+, and N_D^0. For *p*-type semiconductors, $N_D < N_A$, and conductivity in dark is caused by free holes. Under continuous UV illumination, electron-hole pairs are generated at a rate G per unit volume, per second. The concentrations of holes and electrons in steady state conditions are p and n, respectively.

The transition rates of charge carriers among the various states are customarily described as the product of the concentration of charge carriers, the concentration of available empty sites, and a constant representing the capture coefficient.[17,18] Specifically, holes from the valence band are captured by the Mg-related acceptor with a rate $C_{pA}N_A^- p$, and free electrons recombine with these holes at a rate $C_{nA}N_A^0 n$, where C_{pA} and C_{nA} are the hole and electron capture coefficients. Additionally, holes can be thermally emitted from the acceptors to the valence band (*i.e.*, electrons are thermally excited from the valence band to the acceptors) at a rate $Q_A N_A^0$, where

$$Q_A = C_{pA}N_V g^{-1} \exp\left(-\frac{E_A}{kT}\right). \tag{6.1}$$

Here, N_V is the effective density of states in the valence band, and g is the degeneracy factor of the acceptor level (assumed to be equal to 2).[11] If we ignore donor-acceptor pair transitions, the rate equation for transitions through the Mg acceptor for steady-state conditions can be written as,[11]

$$\eta G = C_{pA}N_A^- p - Q_A N_A^0 \ . \tag{6.2}$$

The term on the left side represents the photoluminescence (PL) intensity related to the shallow Mg acceptor, with η being the absolute internal quantum efficiency of the PL. The two terms on the right side represent the capture of free holes by the acceptor and the thermal emission of bound holes to the valence band. Conversely, the PL intensity can also be described as,[11]

$$\eta G = C_{nA}N_A^0 n \, . \tag{6.3}$$

For simplicity, we ignore the donor-acceptor pair transitions, yet they can be accounted for by replacing C_{nA} in Eq. (6.3) with another constant.[11] We also can write the charge neutrality equation:

$$p + N_D^+ = n + N_A^-. \tag{6.4}$$

For low excitation intensity, when $n, p \ll N_A^-, N_D^+$, and $N_D^+ \approx N_D$, then $N_A^- \approx N_D$ and $N_A^0 \approx N_A - N_D$. Then, from Eqs. (6.2) – (6.4), we obtain expressions for the concentrations of free holes and electrons:

$$p = \frac{\eta G}{C_{pA} N_D} + \frac{Q_A (N_A - N_D)}{C_{pA} N_D} = p_0 + p_{th} \tag{6.5}$$

and

$$n = \frac{\eta G}{C_{nA} (N_A - N_D)} \tag{6.6}$$

Interestingly, the concentration of free holes has two components – optical and thermal – whereas the concentration of free electrons has only one component (optical) and is temperature independent. **Figure 15** shows the calculated concentrations of free holes and electrons plotted on a logarithmic scale versus inverse temperature. Concentrations for both low (4 mW·cm^{-2}) and high (30 mW·cm^{-2}) excitation intensity are shown and calculated using Eqs. (6.5) and (6.6). The point at which the concentrations of free holes and free electrons are equal is denoted by $n = p$, and is the temperature at which a conductivity conversion is predicted to occur. To determine the temperature of the conductivity conversion, T_C, we simply multiply the concentrations n and p by the electronic charge and the mobility of electrons and holes. A reasonable but rough

assumption is that electrons have about 10 times greater mobility than holes ($\mu_n / \mu_p \approx 10$), at room temperature.

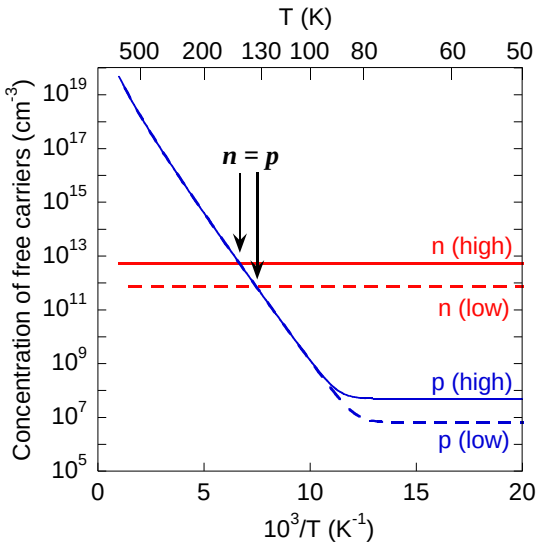

Figure 15: Temperature dependencies of the concentration of free carriers for low (4 mW/cm^2) and high (30 mW/cm^2) excitation power density calculated using Eqs. (6.5) and (6.6) and the following parameters: $N_A = 10^{19}$ cm^{-3}, $N_D = 10^{18}$ cm^{-3}, $N_V = 3.2 \times 10^{15} T^{3/2}$ cm^{-3}, $g = 2$, $\eta = 0.01$, $C_{nA} = 10^{-12}$ cm^3/s, $G = 1.6 \times 10^{23} \times P_{exc}$ cm^{-3}s^{-1}. Arrows at $n = p$ indicate the temperatures at which the concentrations of free holes and free electrons are equal.

At low temperatures, the concentration of free electrons is constant and exceeds the concentration of free holes. The only free holes in the valence band are those that are optically generated, p_0, and can be described by the first term in Eq. (6.5). As the temperature increases, thermally emitted holes, p_{th}, begin to have a significant contribution to the overall concentration of free holes, p, and are described by the second term in Eq. (6.5). At $n = p$, the concentration of free holes is equal to the concentration of free electrons and a switch of the majority charge carrier occurs. Above the temperature of the conductivity conversion, p is greater than n, and p-type conductivity resumes.

From Eqs. (6.5) and (6.6), we solve for T_C by setting the hole- and electron conductivities to be equal:

$$T_C = -\frac{E_A}{k}\frac{1}{\ln\left[\frac{\mu_n}{\mu_p}\frac{\eta g N_D G}{N_V C_{nA}(N_A - N_D)^2}\right]}. \tag{6.7}$$

Using typical parameters for *p*-type GaN (given in the caption of **Figure 15**) and $\mu_n/\mu_p \approx 10$, we calculate that the temperature of conductivity conversion is ~ 150 K and ~ 170 K for two excitation intensities. Experimentally, we see in **Figure 14a** that the temperature of conversion occurs between 110 and 170 K for different GaN samples at P_{exc} = 30 mW/cm^2. In **Figure 14b**, the temperature of conversion is about 130 K and 160 K for the MOCVD-grown sample at 4 and 30 mW/cm^2, respectively. Thus, the theoretical and experimental values for T_C agree qualitatively.

To further understand the mechanism of the conductivity type conversion, it is useful to investigate the characteristic lifetimes of electron and hole transitions through the acceptor. The characteristic time of electron-capture by the acceptor is $\tau_n \approx C_{nA}(N_A - N_D)^{-1}$, and can be roughly estimated to be 10^{-7} s by assuming $C_{nA} = 10^{-12}$ cm^3/s (Ref. 19) and $N_A - N_D = 10^{19}$ cm^{-3}. This value agrees with the PL lifetime for Mg-doped *p*-type GaN which experimentally has been measured to be about 10^{-6} s. Likewise, the characteristic time of hole-capture by the acceptor is $\tau_p \approx (C_{pA}N_D)^{-1} \approx 10^{-12}$ s, assuming that $C_{pA} = 10^{-6}$ cm^3/s (Ref. 19) and $N_D = 10^{18}$ cm^{-3}. Then the ratio of lifetimes, $\tau_n/\tau_p \approx 10^5$. In conjunction with Eqs. (6.5) and (6.6) and at low temperatures (when the p_{th} term can be ignored), it follows that the ratio of carrier concentrations is expressed as,

$$\frac{n}{p} = \frac{\tau_n}{\tau_p} \approx 10^5 \tag{6.8}$$

Equation (6.8) shows that free electrons by far dominate over free holes at low temperatures. Electrons also have higher mobility. Thus, *n*-type conductivity must be observed at low temperatures in *p*-type GaN under UV illumination, and is a direct consequence of the significant difference in the capture rates for free electrons and free holes by the Mg acceptor.

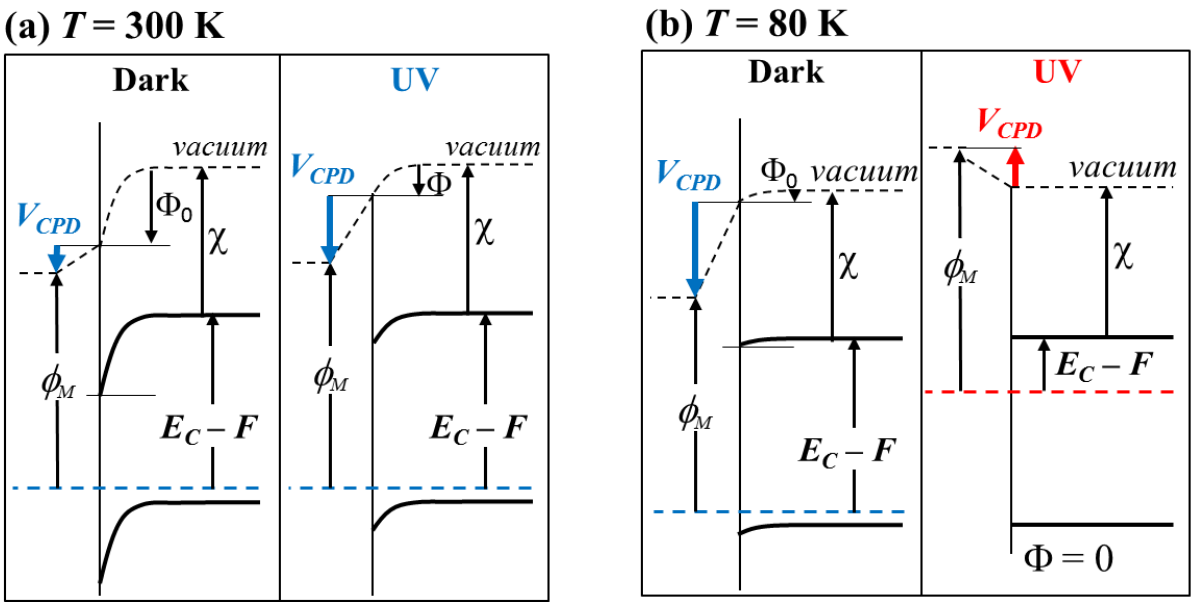

Figure 16: Band diagrams for GaN near the surface to illustrate the reference point used to measure V_{CPD} by the Kelvin probe. (**a**) For T = 300K, the measured change in V_{CPD} is negative and caused by a reduction in the near-surface band bending. (**b**) For T = 80K, the measured change in V_{CPD} is positive and is due to a shift in the quasi-Fermi level for electrons and to *n*-type conductivity.

6.3 Kelvin probe measurements at low temperature

To understand how the conversion of conductivity type affects the actual measurement of the CPD, it is necessary to understand how the Kelvin probe measures the CPD. In **Figure 16**, band diagrams, for T = 300 and 80 K, show that the Kelvin probe measures the CPD as the difference in the work function of the metal probe and the sum of the band bending, the electron

affinity of the semiconductor and the position of the Fermi level in bulk. Under illumination, there are in fact two quasi-Fermi levels: one for electrons and one for holes. Here, we show only the position of the "dominant" Fermi level which corresponds to the carriers with the highest concentration. In both cases, the Fermi level of the metal probe aligns to the position of the dominant bulk Fermi level. The resulting CPD then depends on the band bending value and the position of the Fermi level:[4]

$$qV_{CPD} = \phi_M - \chi - (E_C - F) - \Phi \tag{6.9}$$

It can be shown that illumination of the sample with UV light at low temperatures will significantly decrease the magnitude of the practical band bending. After illumination is ceased, the bands are expected to restore by an insignificant amount, since the restoration of the band bending is temperature dependent.[4] To show that the bands for *p*-type GaN under UV illumination must completely flatten under UV illumination at 80 K, and that the restoration of the band bending is insignificant after illumination has ceased, we may solve for the various flows of free holes from the bulk to the surface. From Eq. (4.1), using parameters given in the caption of **Figure 15**, the rate of holes flowing to the surface, R_{BS}, can be estimated to be about 6×10^{12} $cm^{-2}s^{-1}$ when $\Phi = 0$ and much smaller when $\Phi < 0$. On the other hand, illumination creates about 5×10^{15} $cm^{-2}s^{-1}$ free electrons in the 10 nm-thick near-surface layer when P_{exc} = 30 mW/cm^2. Under illumination, the depletion region and the band bending will decrease until the flow of holes becomes equal to the flow of electrons. To reduce the flow of electrons by three orders of magnitude, the depletion region width and the band bending must decrease by 3 and 6 orders of magnitude, respectively, which essentially means that the band bending is zero. Thus, the flow of holes to the surface is insufficient to compensate the flow of electrons to the surface and the bands are completely flattened under illumination at 80 K.

Additionally, the restoration of band bending in dark is temperature dependent, and the band bending at 80 K is unable to restore to even 0.1 eV within several days. This is because the concentration of free holes in dark is very low at 80 K ($p = p_{th} \approx 10^6$ cm^{-3}) and there is a low probability that they will be able to pass over even a very small near-surface barrier. For our measurements, we wait approximately 10 minutes between illuminations. Therefore, any subsequent UV illuminations after the first illumination should not result in any noticeable SPV since $SPV = \Delta\Phi \approx 0$. However, in stark contrast to these predictions, we actually do observe a substantial change in the CPD signal at 80 K.

From Eq. (6.9), the only parameters which may cause a change in the CPD signal are the band bending and the Fermi-level position:

$$\Delta(qV_{CPD}) = (F_{light} - F_{dark}) - (\Phi_{light} - \Phi_{dark}) = \Delta F - \Delta\Phi \tag{6.10}$$

Taking the change in band bending to be zero, we must conclude that $\Delta V_{CPD} = \Delta F$. Thus, the abnormally large CPD values can only be explained by a change in the position of the Fermi level in bulk. For *p*-type GaN with $E_A \approx 0.2$ eV, the position of the dark Fermi level in bulk, $F - E_V$, is about 0.2 eV for the temperature range $80 < T < 300$ K. However, illumination creates a quasi-Fermi level for electrons which is expected to be close to the conduction band. Since the concentration and conductivity of free electrons are much higher than that of free holes at 80 K under illumination, it is the quasi-Fermi level for electrons that aligns with the Fermi level of the metal probe in our measurements.

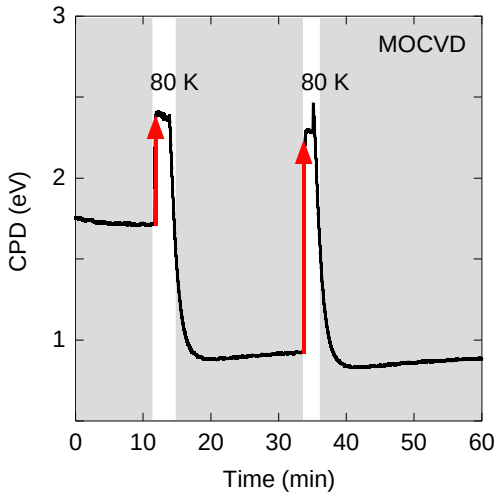

Figure 17: Evolution of the CPD signal in time at 80 K. The first UV illumination occurred after band bending was allowed to fully restore. The CPD baseline changes substantially, and remains unchanged for all subsequent illuminations. The CPD under illumination (within white vertical strips) is 1.5 eV higher than in dark (shadowed areas) due to an upward jump of the quasi-Fermi level for electrons.

6.4 Contact potential difference baseline from low to high temperature

Additional experimental evidence for this change in the Fermi level can be shown by studying the value of the CPD baseline before and after the first UV illumination (*i.e.*, illumination after the bands have reached complete restoration by preheating at 600 K). In **Figure 17**, the CPD of the MOCVD sample is shown. Initially, the value of the CPD in dark is about 1.7 eV but after the first UV illumination, the CPD baseline (dark value) dramatically decreases to ~0.8 eV and remains at this value for all subsequent low-temperature measurements. This change can be attributed to a reduction in the practical downward band bending by about 1 eV after the first illumination. The increase of the CPD signal upon illumination by about 1.5 eV (**Figure 17**) can be explained by the upward shift of the electron Fermi level in bulk by this amount. The point of reference for the Kelvin probe then shifts significantly, and the resulting CPD reflects this change. Although we may qualitatively explain the change in CPD behavior by a shift in the Fermi-level position, the exact value for the position of the Fermi-level cannot be determined. In several measurements for both *n*- and *p*-type GaN, the CPD baseline at

low temperatures is drifting and is inconsistent. At the moment, we are unable to determine the cause of the drift, so the exact calculation of the Fermi-level position remains beyond the scope of this work.

As soon as illumination has ceased, the CPD does not restore instantaneously, but within a few seconds (**Figure 17**). This can be explained by persistent photoconductivity which is observed in Mg-doped GaN,[20,21,22] because the Fermi level is unable to restore to its expected *p*-type value, since a flow of electrons is no longer present to allow for the Fermi level of the semiconductor to align with the work function of the metal probe. It must then reside in some floating state, less than its position under UV, but greater than its restored position in dark. The change in CPD between illumination and dark conditions at 80 K varies for each sample (**Figure 14a**). This is attributed to the fact that the position of the quasi-Fermi level for electrons and the rate of decrease of the electron concentration in the conduction band after switching off illumination may strongly depend on the presence of different defects in the semiconductor. These defects may vary for different growth techniques.

Thus, we see that the behavior for *p*-type GaN is vastly different than its behavior at higher temperatures. At low temperature and under UV illumination, we observe *n*-type SPV behavior for Mg-doped *p*-type GaN. We assume that this *n*-type behavior must be the result of a conversion to *n*-type conductivity due to a higher concentration of free electrons than free holes at low temperatures and under illumination. When the sample temperature is increased, subsequent UV illuminations show that at the temperature T_C, a conversion of the conductivity type occurs, and for increasing temperature, *p*-type conductivity resumes. If the excitation intensity is varied, it is possible to tune the temperature at which the conductivity type conversion occurs.

6.5 Low temperature surface photovoltage in *n*-type GaN

To verify the unique behavior of *p*-type GaN at low temperatures, similar experiments were performed on a degenerate *n*-type GaN sample co-doped with Si and Zn. The sample was grown by MOCVD on c-plane sapphire substrates at the Technische Universitat Braunschweig (TUBS). The concentration of free electrons was found from Hall effect measurements to be 1.0×10^{19} cm^{-3} (Ref. 23). To mimic the experiments performed on the *p*-type samples, this particular sample was heated to 600 K for 1 h before cooling to 80 K with liquid nitrogen, while being in dark conditions.

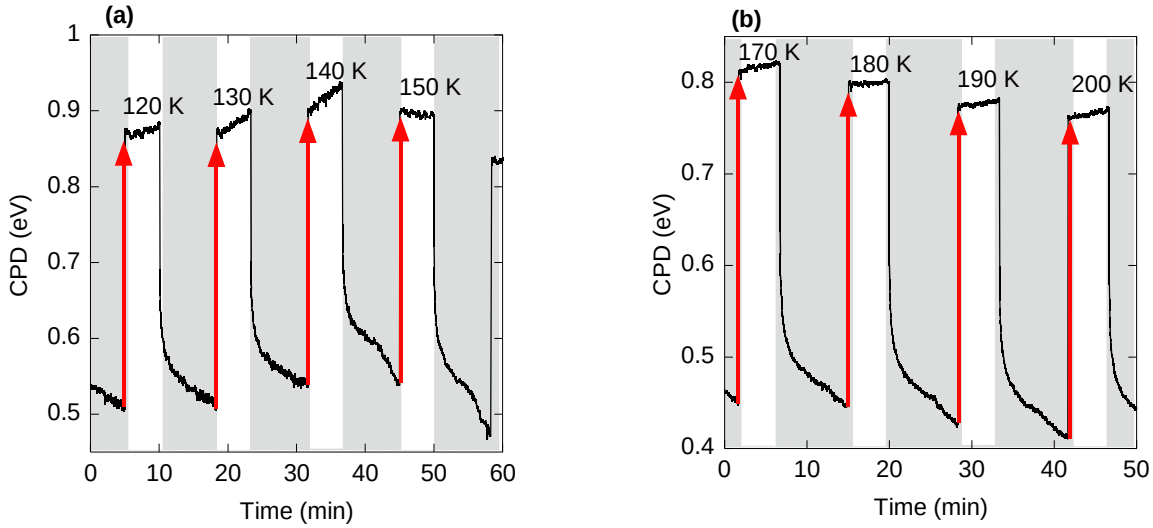

Figure 18: CPD of *n*-type GaN at various temperatures, with P_{exc} = 30 mW/cm^2. (**a**) T < 160 K, and (**b**) T > 160 K. For all temperatures, the SPV exhibits n-type behavior.

Surface photovoltage measurements were performed at various temperatures for about 5 min, beginning at 80 K and increasing to 300 K (in intervals of 10 K), using identical experimental parameters to the *p*-type studies, and are shown in **Figure 18**. The SPV at low temperature displayed "typical" n-type behavior; this is to say, the SPV displayed *n*-type behavior throughout the entire range of temperatures. It is expected for degenerate *n*-type GaN

that the conductivity of the sample does not change in respect to temperature. The SPV results do indeed verify this theory, so we conclude that only *p*-type GaN samples experience a conversion of the conductivity at low temperatures and under UV illumination.

Chapter 7: Photoluminescence in Mg-doped *p*-type GaN

Recent studies of high-resistivity Zn-doped GaN report abrupt thermal quenching of the blue luminescence (BL) band which is tunable by varying the excitation intensity.[11,24] The BL was quenched by several orders of magnitude in a very small temperature range (~10 K) and this phenomenon was attributed to properties of the nonradiative defects in the material. The characteristic temperature at which the quenching occurred increased with increasing excitation intensity; this is to say that the quenching is tunable. From these studies, it was predicted that this quenching should be a general phenomenon, and exhibited in other high-resistivity or *p*-type semiconductors, in particular Mg-doped GaN. Recently, we confirmed this prediction by observing abrupt and thermal quenching of the UV luminescence (UVL) band in Mg-doped *p*-type GaN. Below, the main results of the work reported in Ref. 19 are presented.

7.1 Abrupt and tunable quenching of photoluminescence

Three Mg-doped p-type GaN samples were studied (9591, 9599, 9600), which exhibited two different types of PL behaviors. All the samples were produced by MBE at the Paul-Drude-Institüt fur Festkörperlektronik in Berlin, Germany. They were grown by a two-step process of first growing the substrates and undoped layers, and then growing the Mg-doped layers on top. The concentration of free holes was measured by Hall effect at room temperature and estimated to be $(8.5 \pm 2.5) \times 10^{17}$ cm^{-3}. The concentration of the Mg acceptors was measured by secondary ion-mass spectrometry to be $(3.6 \pm 1.3) \times 10^{19}$ cm^{-3}. The PL was excited using a HeCd laser (40 mW). A more detailed explanation of the experimental setup and procedures can be found in chapter 3.

The absolute internal quantum efficiency of PL, η, is determined from the integrated PL intensity, I^{PL}, of a specific PL band and from the generation rate, G, of electron hole pairs created by the laser per second, per unit volume. The expression for η is given as

$$\eta = \frac{I^{PL}}{G} \ . \tag{7.1}$$

Shown in **Figure 19** are the PL spectra for two characteristic samples (9591 and 9600) for the range of temperatures 20 – 200 K. For both samples, the UVL band at low temperatures dominates the spectrum extending from 2.8 to 3.3 eV and has a maximum at 3.25 eV. Also, there is a weak excitonic band which has a maximum at 3.465 eV at 20 K. Over the range of temperatures, these two representative samples exhibited very different PL behaviors. Thus, we refer to the behavior of sample 9600 as group A, and for the behaviors of 9591 and 9599 as group B.

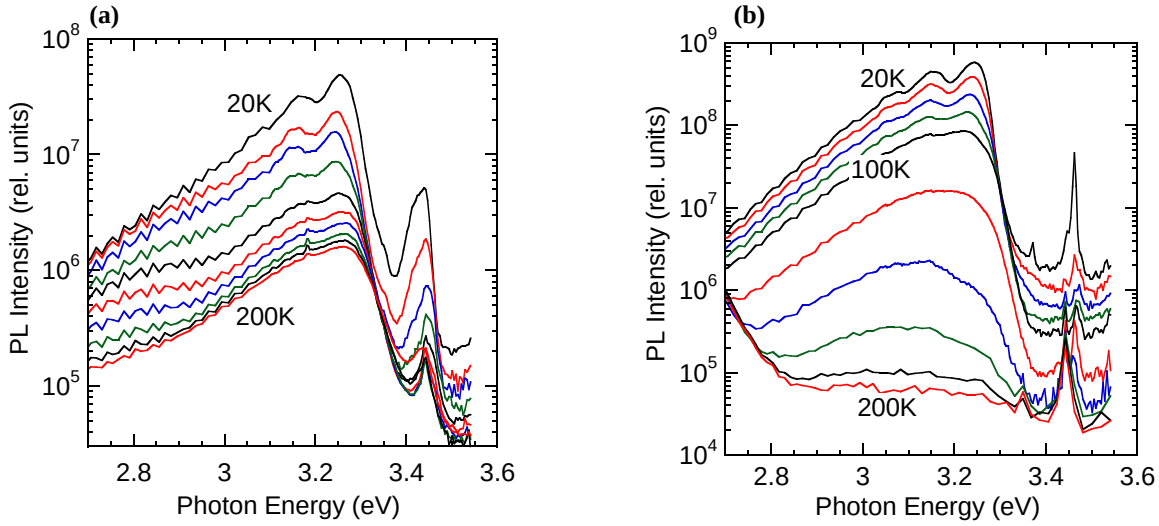

Figure 19: Evolution of the PL spectrum in *p*-type Mg-doped GaN with increasing temperature from 20 to 200 K with step 20 K. (**a**) sample 9600 (group A), (**b**) sample 9591 (group B). P_{exc} = 0.3 W/cm^2. The weak oscillations with a period of about 35 meV are due to a Fabry-Perot effect in the sapphire/GaN/air cavity, revealing the total thickness of the GaN layers (undoped and Mg-doped) to be about 7 μm (Ref.19).

The PL from the UVL band of the group A sample exhibits quenching in the temperature range of 60 – 200 K of only a magnitude in intensity. The activation energy for this quenching was calculated to be about 30 meV. Conversely, the intensity of the UVL band for the group B samples exhibits much more abrupt quenching of about four orders of magnitude in the temperature range of 100 – 180 K. In fact, the UVL band can hardly be distinguished above 200 K in these samples. The temperature at which the quenching occurs, called the characteristic temperature, T_0, is intensity dependent. As the laser intensity is attenuated by neutral density filters, T_0 decreases accordingly, as seen in **Figure 20**. For the sample in group A, however, T_0 appears to be independent of intensity and occurs at a much lower temperature (**Figure 20**).

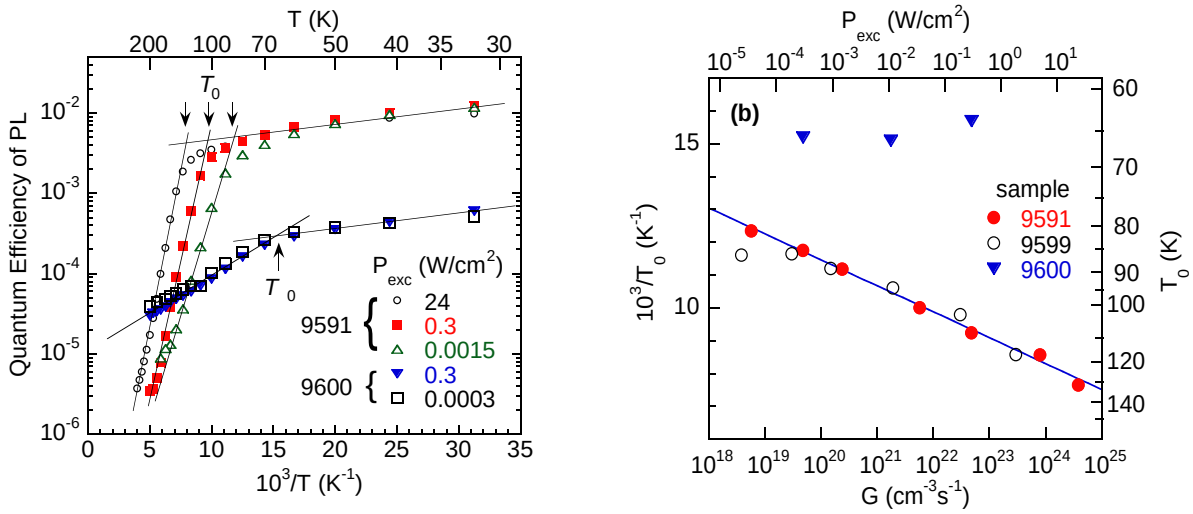

Figure 20: (**a**) Temperature dependence of quantum efficiency of the UVL band in *p*-type Mg-doped GaN for different P_{exc}. Lines are extrapolations of the low-temperature and high-temperature parts with an intersection at the characteristic temperature T_0. For sample 9591 (group B), T_0 shifts with increasing excitation intensity, while for sample 9600 (group A), it does not. (**b**) Dependence of the characteristic temperature T_0 on excitation intensity for the UVL band in three Mg-doped GaN samples. The line is calculated using Eq. (7.2) with E_A = 250 meV and $B = 3\times10^{34}$ cm^{-3}s^{-1} (Ref.19).

When abrupt thermal quenching was observed in high-resistivity Zn-doped GaN, it was postulated that the system must undergo a conductivity conversion for temperatures below the

quenching temperature, and revert to its normal state above the quenching temperature. This model is similar in some respects to the model which we invoke to explain the change in conductivity of the *p*-type samples studied in the previous chapter of this work. We will discuss the similarities and differences in a subsequent section.

To understand the behavior of T_0, we can plot 1/ T_0 as a function of the logarithm of the excitation intensity, and by using the relation,[11]

$$T_0 \approx T^* = \frac{E_A}{k \ln(B/G)} , \tag{7.2}$$

with,

$$B = C_{pA}(\eta_0^{-1} - 1)(N_A - N_D)N_V / 2 . \tag{7.3}$$

Here, E_A is the activation energy of the acceptor A responsible for the abrupt quenching of PL, C_{pA} is the hole capture coefficient for the acceptor, η_0 is the internal quantum efficiency of PL through the acceptor A at temperatures below T_0, N_A and N_D are the concentrations of the acceptor and shallow donor, respectively, and N_V is the effective density of states in the valence band. In **Figure 20b**, we see that there is a linear dependence between the logarithm of the excitation intensity and the inverse of the characteristic temperature.

The temperature and intensity dependencies for sample 9591 were studied in more detail, and the quantum efficiency of the PL is plotted for a wide range of excitation intensities in **Figure 21**. The quenching is fit numerically using the model and Eqs. (7) – (12) from Ref. 11. These calculated fits agree qualitatively with the experimental data and do reproduce the tunable quenching effect for the UVL band. Although, the fits are not exact, they illustrate clearly that T_0 shifts to higher temperatures at higher intensities as predicted by Eq. (7.2).

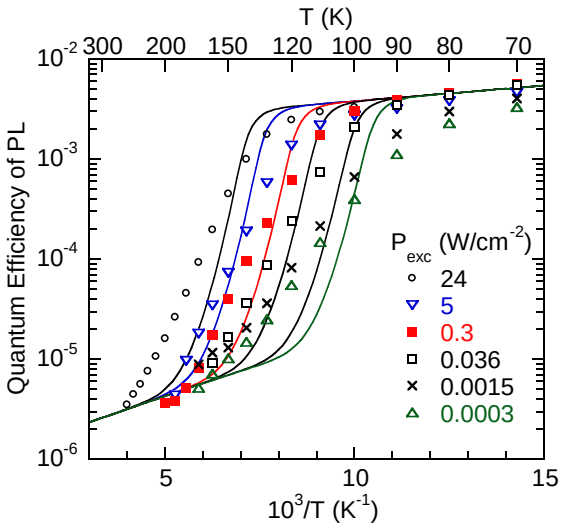

Figure 21: Temperature dependence of quantum efficiency of the UVL band in *p*-type Mg-doped GaN (sample 9591) for excitation power densities between 3×10^{-4} and 24 W/cm^2. Solid lines are numerical solution of Eqs. (5)-(10) from Ref. 11 with the following parameters: $N_S = 9\times 10^{18}$ cm^{-3}, $N_A = 2\times 10^{19}$ cm^{-3}, $N_D = 1\times 10^{17}$ cm^{-3}, $C_{nD} = 8\times 10^{-8}$ cm^3/s, $C_{nS} = 10^{-6}$ cm^3/s, $C_{pS} = 5\times 10^{-6}$ cm^3/s, $C_{pA} = 10^{-6}$ cm^3/s, $C_{DA} = 10^{-11}$ cm^3/s, $C_{nA} = 10^{-12}$ cm^3/s, $E_D = 10$ meV, $E_A = 270$ meV, $G = 1.6 \times 10^{23} \times P_{exc}$ cm^{-3}s^{-1} (Ref.19).

The slope of the fits increases from 100 to 180 meV as the excitation intensity increases from 10^{-3} to 24 W/cm^2. The capture coefficients assumed for these fits are within an order of magnitude of the previously calculated values for the BL band in the high resistivity Zn-doped GaN samples. Interestingly, the concentrations of the acceptor and the nonradiative deep donor are higher than in the Zn-doped samples; however, this outcome is expected since to obtain reliable *p*-type GaN, the samples are heavily doped with Mg. The calculated ionization energy of the Mg acceptor is about 250 – 270 meV which is larger than the previously reported values for Mg-doped GaN [150 – 200 meV (Ref. 9)]. This discrepancy is preliminarily attributed to potential fluctuations which are prevalent in heavily doped or compensated acceptors such as are in Mg-doped GaN.

7.2 Phenomenological model of the abrupt and tunable quenching

To explain the abrupt quenching of the PL for the group B samples, we use a phenomenological model involving three defects which participate in the recombination of photo-generated carriers.[11] The first defect is the Mg acceptor (Mg_{Ga}) which contributes to the UVL band. A second defect is the shallow donor which may possibly be O_N or V_NH.[25] Electron transitions from this donor to the acceptor are considered to be the main contributor of the UVL band, for low temperatures. A third defect must be included since the quantum efficiency through these two channels is much less than 100%. We assume the presence of an additional donor with a deep level in the band gap which participates in nonradiative recombinations. In the previous report on abrupt thermal quenching,[11] the same set of defects was used to explain the behavior; however, the nonradiative defect may differ between the high resistivity samples and these *p*-type samples.

At low temperatures ($T < T_0$), the model predicts that the nonradiative, *S*, centers are completely filled with electrons immediately as the sample is illuminated with UV light. This results in the accumulation of electrons in the conduction band since the recombination rate of electrons through the acceptor is very slow. The build-up of electrons in the conduction band produces *n*-type conductivity. For temperatures above the quenching temperature ($T > T_0$), holes from the Mg acceptor receive enough thermal energy to be excited to the valence band. These free holes efficiently recombine with electrons in the *S* center, which re-opens the channel and allows for the excess electrons in the conduction band to be compensated. Since a majority of the recombinations are occurring through the very efficient *S* center, donor-acceptor pair transitions decrease dramatically for $T > T_0$. The process of holes being emitted to the valence band over a range of temperatures is what triggers the process of quenching. With the increase in the

concentration of free holes in the valence band at higher temperatures, *p*-type conductivity resumes.

Finally, we note that this quenching behavior only occurs for the group B samples and is not observed for the other type of samples. We may preliminarily attribute this effect to the presence of different nonradiative centers for the different samples. Further research into the properties of these defects should elucidate some of the unexplained behaviors.

7.3 Comparison of the photoluminescence and Kelvin probe models

To show that different types of nonradiative defects may result in different temperature dependencies of the PL in Mg-doped GaN samples, we varied the parameters of the nonradiative center *S* within the phenomenological model which includes three types of defects.

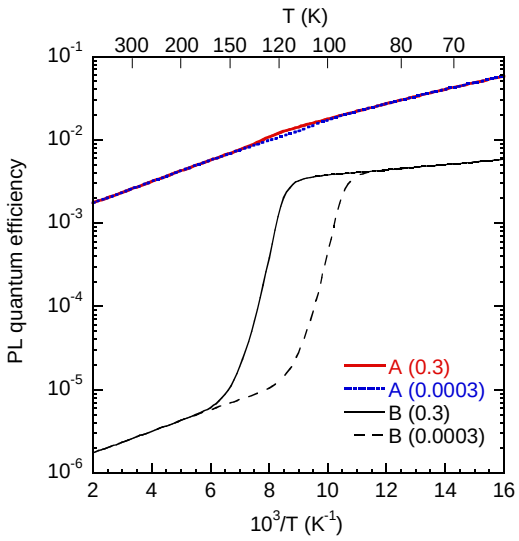

Figure 22: Calculated temperature dependencies of the PL quantum efficiency for the UVL band in Mg-doped GaN. A and B are two groups of samples for which we have varied the properties of the nonradiative defect *S*. Excitation power density is 0.0003 and 0.3 W/cm^2. The model parameters for the group B sample are given in the caption to **Figure 21**. Parameters for the group A sample are $C_{nS} = 10^{-9}$ cm^3/s and $C_{pS} = 10^{-3}$ cm^3/s, and any other parameters are the same as for sample B.

In **Figure 22**, the temperature dependencies for the PL quantum efficiency of the UVL band in the Mg-doped GaN samples (group B as described in Ref. 15) are plotted as thin solid and dashed curves. The dependencies exhibit an abrupt and tunable quenching. The abrupt quenching is observed at $T_0 \approx 100$ K for $P_{exc} = 0.0003\,\mathrm{W/cm^2}$ and at $T_0 \approx 125$ K for $P_{exc} = 0.3\,\mathrm{W/cm^2}$. By varying the parameters of only the nonradiative center in this model (specifically, increasing C_{pS} and decreasing C_{nS}) we are able to reproduce qualitatively the temperature behavior for the samples of group A (namely, a small activation energy of the thermal quenching and the absence

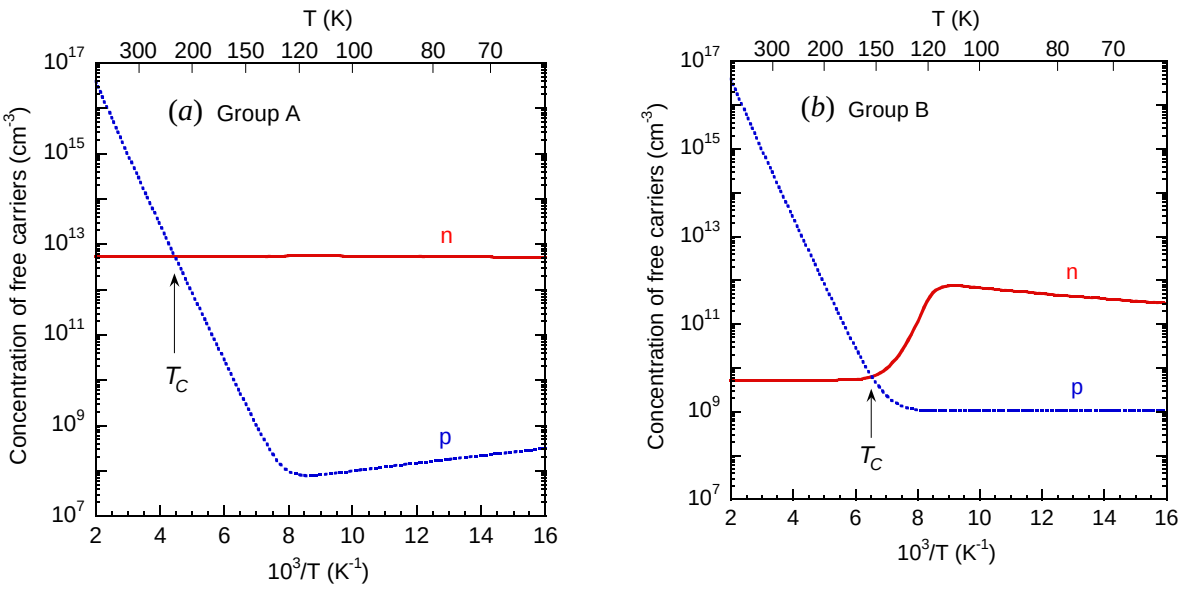

Figure 23: Calculated temperature dependencies of the concentration of free electrons and holes in Mg-doped GaN samples of group A (**a**) and group B (**b**). Arrows indicate the temperatures at which $n = p$ and at which conduction type is converted if the electron and hole mobilities are equal. (**a**) T_C = 225 K and (**b**) T_C = 155 K. Model parameters are the same as in **Figure 22**. P_{exc} = 0.3 W/cm^2.

of tunability.)

Now, to compare this PL behavior with our Kelvin probe results, we may analyze the temperature dependencies of the concentrations of free electrons and holes for these two sample groups. **Figure 23** and **Figure 24** show these dependencies for both groups of samples for P_{exc} = 0.3 and 0.0003 W/cm^2, respectively.

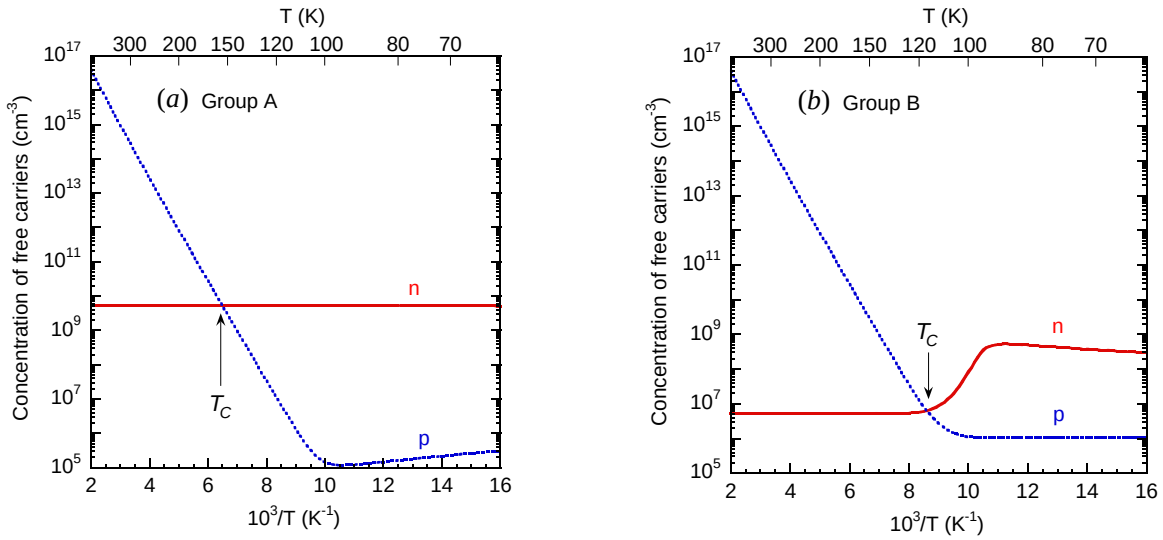

Figure 24: Same as in **Figure 23** except for P_{exc} = 0.0003 W/cm^2. (**a**) T_C = 155 K and (**b**) T_C = 115 K. Model parameters are the same as in **Figure 22**.

We can see from **Figure 23** and **Figure 24** that for both groups of samples, a conversion of the conductivity type and a tunability with excitation intensity of the characteristic conversion temperature are observed. This shows that by varying the properties of the nonradiative defect, we can observe different PL quenching behavior, but always observe a conversion of conductivity as measured by the Kelvin probe for different p-type GaN samples grown by various techniques. The different values of T_C between the samples of group A and B (as shown in **Figure 23** or **Figure 24**) can also explain the sample dependent nature of T_C in the Kelvin probe measurements (see **Figure 14**).

In summary, we have shown both experimentally and theoretically that the properties of the defects in *p*-type GaN dictate the PL behavior in terms of quenching and tunability, as well as the conductivity type of the sample at low temperatures and the dependence of the characteristic temperature of conversion on illumination intensity.

Chapter 8: Conclusions

This thesis has discussed the temperature dependent behavior of both *n*- and *p*-type GaN by investigating the optical and electronic properties through Kelvin probe SPV and PL studies. For high temperatures, the Kelvin probe SPV data show that the band bending in the representative *n*- and *p*-type GaN samples is constant through a wide range of temperatures, and the accurate value of band bending can only be measured if the band bending is allowed to restore at sufficiently high temperatures or periods of time. Furthermore, we investigated the SPV behavior of *n*- and *p*-type GaN at low temperatures. The *n*-type SPV behavior for heavily doped, degenerate GaN remains consistent even at low temperatures. Conversely, we observe that at low temperatures, *p*-type Mg-doped GaN exhibits a conversion in conductivity from *p*- to *n*-type as the temperature is decreased below a characteristic temperature, T_C. We attribute this to a switch in the majority charge carriers under UV illumination. The temperature of the conductivity conversion is tunable with excitation intensity. Finally, PL studies show abrupt and tunable thermal quenching of the UVL band in some Mg-doped GaN samples. This effect is also explained by a conductivity conversion, but with additional centers participating in the recombination processes. Specifically, a nonradiative center with a high capture rate of electrons is necessary to explain the abrupt and thermal quenching. Interestingly, we assert that the properties of this center may be the explanation for why the quenching is observed for some Mg-doped samples and not for others. Also, this is the pivotal reason why a conversion of conductivity resulting in *n*-type SPV behavior at low temperatures should occur for any *p*-type GaN sample, whereas abrupt thermal quenching of PL may only occur for some samples.

In summary, studying the optical and electronic behaviors of GaN through Kelvin probe SPV studies and PL studies may shed light on the properties of defects in GaN and their effect on the overall performance of GaN-based devices and materials.

References:

[1] Navigant Consulting, U.S. Lighting Market Characterization (U.S. Department of Energy, Office of Building Technologies, http://www.eere.energy.gov/, September, 2012).

[2] J. P. Long and V. M. Bermudez, *Phys. Rev. B.* **66**, 121308 (2002).

[3] M. Eyckeler, W. Monch, T. U. Kampen, R. Dimitrov, O. Ambacher, and M. Stutzmann, *J. Vac. Sci. Technol. B* **16**, 2224 (1998).

[4] M. A. Reshchikov, M. Foussekis, A. A. Baski, *J. Appl. Phys.* **107**, 113535 (2010).

[5] M. Foussekis, J.D. McNamara, A. A. Baski, M. A. Reshchikov, *Appl. Phys. Lett.* **101**, 082104 (2012).

[6] L. Kronik and Y. Shapira, *Surf. Sci. Rep.* **37**, 1, (1999).

[7] I. D. Baikie, K. O. van der Werf, H. Oerbekke, J. Broeze, and A. van Silfhout, *Rev. Sci. Instrum*. **60**, 930 (1989).

[8] J. D. McNamara, M. Foussekis, H. Liu, H. Morkoc¸, M. A. Reshchikov, and A. A. Baski, *Proc. SPIE* **8262**, 826213 (2012).

[9] M. A. Reshchikov and H. Morkoç, J. Appl. Phys. **97**, 061301 (2005).

[10] J. P. Long and V. M. Bermudez, *Phys. Rev. B* **66**, 121308 (2002).

[11] M. A. Reshchikov, A. Kvasov, T. McMullen, M. F. Bishop, A. Usikov, V. Soukhoveev, and V. A. Dmitriev, *Phys. Rev. B* **84**, 075212 (2011).

[12] McCallister Technical Services, Kelvin probe user manual, (1999-2007).

[13] D. C. Look, C. E. Stutz, R. J. Molnar, K. Saarinen, and Z. Liliental-Weber, *Sol. St. Comm*. **117**, 571 (2001).

[14] K. M. Tracy, W. J. Mecouch, R. F. Davis and R. J. Nemanich, *J. Appl. Phys*. **94**, 3163 (2003).

[15] P. Ščajev, K. Jarašiūnas, S. Okur, Ü. Özgür, and H. Morkoç, *J. Appl. Phys*. **111**, 023702 (2012).

[16] H. Nienhaus, M. Schneider, S. P. Grabowski, W. Monch, R. Dimitrov, O. Ambacher, and M. Stutzmann, *Mater. Res. Soc. Symp*. Proc. **680**, E4.5 (2001).

[17] V. N. Abakumov, V. I. Perel, and I. N. Yassievich, *Nonradiative Recombinations in Semiconductors* (Elsevier, Amsterdam, 1991).

[18] W. Shockley and J. W. T. Read, *Phys. Rev.* **87**. 835 (1952).

[19] M. A. Reshchikov, J. D. McNamara, S. Fernández-Garrido, and R. Calarco, *Phys. Rev. B* **87**, 115205 (2013).

[20] C. H. Qiu and J. I. Pankove, *Appl. Phys. Lett*. **70**, 1983 (1997).

[21] J. Z. Li, J. Y. Lin, H. X. Jiang, A. Salvador, A. Botchkarev, and H. Morkoç, *Appl. Phys. Lett*. **69**, 1474 (1996).

[22] C. Johnson, J. Y. Lin, H. X. Jiang, M. Asif Khan, and C. J. Sun, *Appl. Phys. Lett*. **68**, 1808 (1996).

[23] M. A. Reshchikov, M. Foussekis, J. D. McNamara, A. Behrends, A. Bakin, and A. Waag, *J. Appl. Phys.* **111**, 073106 (2012).

[24] M. A. Reshchikov, *Phys. Rev. B* **85**, 245203 (2012).

[25] O. Gelhausen, M. R. Phillips, E. M. Goldys, T. Paskova, B. Monemar, M. Strassburg, and A. Hoffmann, Mater. Res. Soc. Symp. Proc. **798**, Y5.20 (2004).